MAGPIE

SMART GREEN PORTS

Smart Energy Demonstrator Report



Funded by the European Union

This project has received funding from the European Union's Horizon 2020 (MFF 2014-2020) research and innovation programme under Grant Agreement 101036594

D3.13 – Smart Energy Demonstrator Report

Grant Agreement No.	101036594
Start date of Project	1 October 2021
Duration of the Project	60 months
Deliverable Number	D3.13
Deliverable Leader	EUR
Dissemination Level	PU
Status	V.1.0
Submission Date	01-12-2025
Author	Neda Vahabzad (n.vahabzad@tudelft.nl) Pedro Vergara Barrios (P.P.VergaraBarrios@tudelft.nl)

This project has received funding from the European Union's Horizon 2020 research and innovation programme under grant agreement No 101036594.

The opinions expressed in this document reflect only the author's view and in no way reflect the European Commission's opinions. The European Commission is not responsible for any use that may be made of the information it contains.

Modification Control

Version #	Date	Author	Organisation
1.0.	01-12-2025	Neda Vahabzad, Pedro Vergara Barrios	TU Delft
2.0.	23-07-2026	Neda Vahabzad, Pedro Vergara Barrios	TU Delft

Release Approval

Name	Role	Date
André Lisboa	WP Leader	17-12-2025
Yves-Marie Bourrien	Peer reviewer	20-2-2026
Maaike Dalhuisen	Peer reviewer	14-2-2026
Maarten Flikkema	Scientific coordinator	13-9-2026
Arne-Jan Polman	Coordinator	14-9-2026

1. Table of Contents

Abbreviation 5
Executive Summary 6
1. Introduction 8
2. Smart energy systems simulator 10
2.1 Overview 10
2.2 Simulator 10
2.2.1 Description of the model 10
2.2.2 Inputs/Outputs 10
2.3 Scenario generation tool 12
2.3.1 Description of the model 12
2.3.2 Inputs/Outputs 15
2.4 Grid assessment module 16
2.4.1 Description of the model 16
2.4.2 Inputs/Outputs 17
2.5 Summary of tool capabilities, implementation, and accessibility 18
3. Case study-Port of Sines 19
3.1 Overview 19
3.2 Energy transition plans in Port of Sines 23
4. Results 27
4.1 Generated scenarios 27
4.2 Base case analysis 28
4.3 MC simulations 33
4.4 KPI calculations 37
4.4.1 Technical (Demo-specific) KPIs 38
4.4.2 General KPIs 47
5. Conclusions & Next steps 52

Abbreviation

WP, work package

SESST, Smart energy systems simulator tool

KPI, Key Performance Indicators

RES, Renewable energy sources

ESS, Energy storage systems

DSO, Distribution system operator

DER, Distributed energy resources

CGMES, Common grid model exchange standard

PV, Photovoltaic

PF, Power flow

MC, Monte Carlo

Q, Quarter

KNN, K-Nearest Neighbors Regression

FDA, Functional data analysis

APS, Administration of the Port of Sines

MV, Medium-voltage

OPS, Onshore power supply

EMS, Energy monitoring service

REC, Renewable energy community

Executive Summary

With the anticipated growth in electricity demand driven by electrification, heating, and digitalization, accurate load forecasting has become essential for distribution system operators (DSOs), planners, and policymakers to support timely grid development, congestion management, and infrastructure planning. To address this need, Demo 2 of the MAGPIE project (WP3.8) develops a Smart Energy Systems Simulator Tool (SESST) that combines a scenario generation tool for creating realistic 2030 and 2050 demand profiles with a grid assessment module for evaluating distribution grid performance under future scenarios.

The SESST evaluates electrical grid performance under current and future configurations incorporating renewable energy sources (RES), energy storage systems (ESS), and planned grid extensions. It provides key performance indicators (KPIs) to identify congestion risks and flexibility needs while supporting investment planning and decision making. Designed as a generalized and scalable platform, it can be applied to different grid models, datasets, and planning contexts.

The main objectives of this task can be summarized as follows:

- Develop a scenario generation tool to forecast realistic future demand profiles.
- Model current and future grid configurations, including RES, ESS, and planned network extensions.
- Develop a scalable SESST to assess grid performance, identify congestion, flexibility needs, synergies, and barriers, and provide decision-support KPIs.

This document begins with an introduction to Demo 2, outlining the motivation, objectives, and associated deliverables. Section 2 presents the Smart Energy Systems Simulator Tool (SESST), including the scenario generation tool and grid assessment module, together with their main components, inputs, outputs, and usage. Section 3 presents the Port of Sines case study used to validate the tool and demonstrate its capabilities. Although the validation is based on the Port of Sines, the SESST is designed as a generalized and scalable framework that can be applied to various industrial grids and electrical network configurations. Finally, Section 4 summarizes the main findings, key insights, and recommendations for future work.

Table 1 summarizes the key research questions addressed in Demo 2, grouped into the grid assessment module and the scenario generation tool.

Based on the Demo implementation and analyses, the following recommendations are identified to support (i) tool development and management and (ii) deployment through governance and stakeholder engagement.

1. Facilitating and managing the development process

- Establish transparent data access protocols and validate modelling assumptions with industry experts.
- Reliable data-sharing platforms with clarified data ownership, especially when coordinating among multiple stakeholders (e.g., distribution system operator (DSO)s, distributed energy resource (DER)s operators, port authorities).
- Adopt standardized data formats (e.g., CGMES/CIM) Common Information Model (CIM) for Grid Models Exchange), to improve interoperability and data integration.

Table 1. Research aspects and analytical focus areas of Demo 2

Sector	Questions
Grid assessment module	1. What are the key operational challenges and limitations in the current grid, and which areas show the highest potential for upgrades or extensions? 2. How does the grid perform under future configurations and generated scenarios, and what congestion challenges, flexibility requirements, synergies, and barriers emerge from these analyses? 3. What methods and simulation approaches can be used to analyze and evaluate grid operation and performance repeatedly under multiple generated energy scenarios?
Scenario generation tool	1. What methodologies can be applied to accurately forecast future energy demand using historical data? 2. Which forecasting techniques are most suitable for generating realistic time-series demand profiles rather than single-point estimates? 3. What input data and parameters are essential for developing an accurate and adaptable energy demand forecasting model?

2. Governance support and stakeholder engagement

- Institutional support and technical coordination should be promoted through governance mechanisms or formal policies to ensure the consistent and scalable deployment of the scenario generation and grid assessment tools, while supporting role clarification, workflow integration, and stakeholder capacity building.
- Strengthen digitalization through improved data management, real-time monitoring, and decision-support capabilities.
- Maintain close collaboration with energy-sector stakeholders to validate assumptions and ensure operational relevance.
- Provide training to enable effective use of the tool by stakeholders with varying levels of technical expertise.

Key Insights

The key insights provided by the tool from different perspectives, including grid operators, the Port of Sines authority, energy planners, and other relevant decision-makers, are summarized as follows:

1. Planning future grid investments and expansions

- Strategic investment planning: The tool identifies spatial and temporal congestion risks, helping prioritize grid reinforcements and support evidence-based investment decisions.
- Investment alignment: Early identification of congestion supports coordinated grid and electrification investments aligned with long-term decarbonization goals.

2. Social acceptance and broader use cases

- Multi-stakeholder value: The Demo demonstrated that the tool provides decision-support information for DSOs, port authorities, large energy consumers, DER owners, investors, and public institutions. The results highlighted that different stakeholders can extract decision-relevant information from the same analysis framework, depending on their perspective.
- Improved coordination: Transparent visualization of congestion risks and future capacity constraints provides a common basis for coordinated planning toward the development of congestion-resilient and sustainable energy infrastructure.

In summary, the Demo demonstrated that successful deployment of the scenario generation and grid assessment tools depends not only on technical robustness but also on effective data governance, institutional coordination, and stakeholder engagement. This insight emerged from the practical challenges encountered during the case study development. In particular, The transition from the Port of Rotterdam to the Port of Sines due to data availability highlighted the importance of transparent data-sharing protocols, standardized formats, and early coordination with data-owning entities are essential preconditions for successful tool deployment. When these conditions are met, the tools can effectively support long-term grid planning, investment decisions, and stakeholder collaboration for resilient and sustainable energy systems.

Demo 2 is led by Neda Vahabzad (n.vahabzad@tudelft.nl), and Pedro Vergara Barrios (P.P.VergaraBarrios@tudelft.nl) from TU Delft. The scenario generation tool is being developed in collaboration with Yashar Ghiassi-Farrokhfal (y.ghiassi@rsm.nl), and Adrian Esteban Perez (estebanperez@rsm.nl) from Erasmus University Rotterdam (EUR).

The developed scenario generation and grid assessment tools are intended as planning tools rather than real-time operational systems. By combining demand scenario generation with grid feasibility assessment, they support long-term infrastructure planning, stakeholder coordination, and investment decisions under uncertainty.

1. Introduction

Ports are energy-intensive and high-emission hubs and critical nodes in global trade and transportation. Their operations involve extensive use of fossil fuels for shipping, cargo handling, and on-site logistics, contributing significantly to greenhouse gas emissions and local air pollution. As international climate targets tighten and environmental regulations become more stringent, the transition toward green ports has gained increasing importance.

Green ports aim to pursue the decarbonization of port-related activities through the integration of alternative fuels and sustainable technologies, including large-scale electrification, hydrogen-based solutions, and biofuels. While these measures significantly reduce emissions, they also create new challenges for the port's electrical infrastructure. The increasing electrification of transport systems, cargo handling equipment, shore power (cold ironing) for berthed vessels where applicable, and other auxiliary systems leads to higher energy demand and grid stress, requiring more flexible and reliable power distribution systems.

The electrical network of a green port can be considered as a microgrid, due to its geographically confined structure evolving through the integration of diverse local generation units including DERs and RESs such as Photovoltaic (PV) systems, wind turbines, and ESSs, as depicted in Figure 1. Although these technologies enhance sustainability and

operational flexibility, they also introduce technical challenges, including bidirectional power flow (PF), variability in generation and demand profiles, and an increased risk of congestion. The term bidirectional power flow refers to the situation in which locally generated power from DERs exceeds local demand and is exported to the upstream grid, while at other times power is imported from the grid to supply loads.

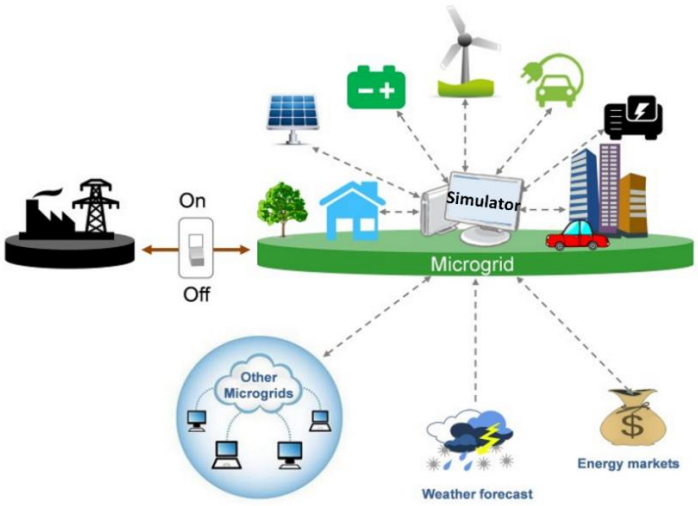


Figure 1. A modern microgrid equipped with multiple DER and RES technologies.

The port is used as a representative case study within the context of the MAGPIE project. However, the proposed modeling and optimization framework is not limited to port applications and is generally applicable to any distribution network or microgrid with high DER penetration.

As energy infrastructures evolve toward more decentralized and interactive architectures with multiple stakeholders, systematic performance assessment becomes essential. Their operation must be evaluated under both short-term operational conditions and long-term development scenarios to ensure reliable, efficient, and economically sound performance. This requires the simulation of grid behavior under prospective conditions that incorporate infrastructure expansions, such as additional DER integration, network reinforcements, and line extensions, as well as projected demand growth.

From a broader system perspective, including technical, economic, planning, and policy dimensions, a simulation and decision-support tool can support stakeholders ranging from grid operators and port authorities to planners, policymakers, and investors. Such a framework facilitates the evaluation of alternative development pathways, enables the early identification of operational challenges, and supports informed decision-making consistent with sustainability, resilience, and decarbonization goals.

2. Smart energy systems simulator

2.1 Overview

Transition toward greener and more electrified port operations introduces several challenges for the electrical infrastructure, including increased load demand, grid congestion, and the need for enhanced flexibility to accommodate variable renewable generation. To address these challenges, the SESST has been developed to model and simulate the port's electrical infrastructure under both current and future conditions. The tool enables the evaluation of system performance, identification of flexibility requirements and congestion risks, and assessment of opportunities for integrating additional green technologies. By incorporating realistic demand growth scenarios, SESST provides accurate and forward-looking analyses of grid behavior. It serves as a decision-support tool for both grid operators and investors, offering insights into realistic demand scenarios, congestion risks, potential synergies, and operational constraints.

2.2 Simulator

To maximize its applicability, SESST has been designed as a generalized and scalable model rather than a case-specific tool. Its modular structure enables adaptation to different datasets, system configurations, and geographical contexts, allowing application to other case studies, including ports, industrial clusters, and regional energy systems. The framework can represent varying grid topologies, technology portfolios (e.g., electrification, hydrogen, storage), and development scenarios. This flexibility ensures that SESST can support both future research and practical decision-making processes across diverse energy infrastructures and transition pathways.

2.2.1 Description of the model

Demo 2 of the MAGPIE project focuses on developing the SESST, designed to model and simulate the operation of a port electrical infrastructure under both current conditions and future development scenarios. The SESST framework is composed of two main components that work in sequence to provide a comprehensive analysis of grid behavior and performance, including:

1) Scenario generation tool: This component forecasts future energy demand profiles for target years such as 2030 and 2050 using historical and contextual data.
2) Grid assessment module: This component models the electrical distribution network (of the Port of Sines), incorporates planned infrastructure expansions, and performs detailed technical simulations. It integrates PF analysis and Monte Carlo (MC) (download) simulations to evaluate voltage profiles, line loadings, and operational feasibility under deterministic scenarios. In addition, Monte Carlo (MC) simulations are applied to capture uncertainty in demand growth, renewable generation, and technology deployment. The combination of PF and MC methods enables both deterministic technical validation and probabilistic assessment of congestion risks and flexibility requirements, resulting in robust KPIs for system operation and long-term planning.

2.2.2 Inputs/Outputs

Fout! Verwijzingsbron niet gevonden. illustrates the overall structure of SESST, highlighting the workflow, key inputs, and resulting outputs of each component. The scenario generation tool uses training datasets such as weather conditions, historical load demand, and electricity prices to generate forecasted energy demand profiles for future target years (e.g., 2030 and 2050). Weather data are included to capture the variability of renewable

generation and temperature-dependent demand, historical load data provide the baseline consumption patterns, and electricity prices enable the representation of market-driven behavioural effects.

In this study, all three datasets are required due to the forecasting methodology implemented in the scenario generation model. The adopted forecasting approach explicitly links demand evolution to weather-dependent patterns and price-responsive behaviour; therefore, historical load data alone would not adequately capture seasonal variability or behavioural shifts. The combination of load, weather, and price inputs constitutes the minimum dataset necessary to produce realistic, seasonally consistent demand projections suitable for subsequent Monte Carlo simulations and grid assessment.

The grid assessment module takes as input the characteristics of the port's electrical grid, including its topology, generation assets, demand profiles, and price data. Through its Python-based (Welcome to Python.org) simulation environment, it performs MC and AC PF analysis to assess the system's operational performance under various configurations and scenarios. The module's outputs are categorized into two groups:

- Grid Insights: grid performance indicators and identification of operational bottlenecks and potentials.
- Decision Support: flexibility requirements, congestion risk analysis, and decision-support KPIs such as renewable curtailment and asset utilization under congestion.

The final outcome is a modular and scalable simulation model capable of adapting to different datasets and case studies, supporting comprehensive assessment of grid operation, flexibility needs, and congestion risks under various future conditions.

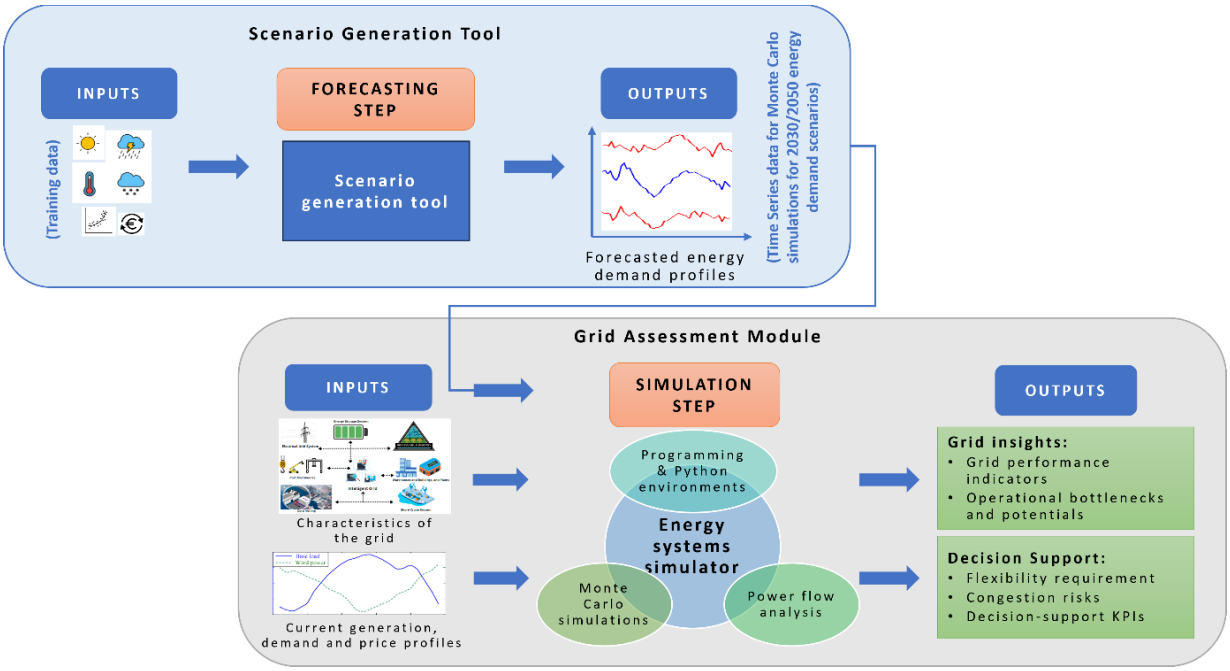


Figure 2. SESST and its components: 1. Scenario generation tool, 2. Grid assessment module.

2.3 Scenario generation tool

2.3.1 Description of the model

The scenario generation tool is designed to generate a set of plausible future energy demand profiles. Historical load demand data from the case study is used as a structural baseline to preserve realistic daily and seasonal demand patterns, including peak timing, ramping behavior, and spatial correlations within the network. It is obvious that the future energy system will differ significantly from today due to electrification of transport and heating, increased DERs, and evolving flexibility mechanisms. Therefore, historical data is not used as a direct forecast of future demand levels, but rather as a validated template that captures intrinsic load dynamics.

Future-oriented adjustments are incorporated through variability in weather conditions, day-ahead electricity prices, and scenario-based scaling assumptions consistent with projected system developments. The Functional Data Analysis (FDA) approach enables the generation of smooth, diverse, and internally consistent demand patterns for a given month, while maintaining realistic temporal structures. The main advantage of this approach is that it combines operational realism with forward-looking adaptability. A limitation is that disruptive structural shifts or entirely new consumption patterns may not be fully represented; therefore, results should be interpreted within the defined scenario assumptions for 2030 and 2050.

The objective of the scenario generation tool is to generate daily energy demand profiles for the years 2030 to 2050, taking seasonal variations into account by allowing users to select a specific month. Each three-month period is grouped into one quarter (Q), representing one of the four main seasons of the year (Q1: January–March, Q2: April–June, Q3: July–September, Q4: October–December). For a selected month, the model generates multiple daily demand scenarios, where each scenario consists of a full 24-hour load profile represented at hourly resolution. Rather than producing independent hourly demand values, the approach generates a complete daily demand curve in each run. This ensures that temporal correlations between hours, such as morning ramp-ups, midday variations, and evening peaks, are preserved. Each scenario is represented as functional data, meaning the 24-hour load profile is modeled as a continuous function. This functional representation maintains smoothness and realistic intra-day dynamics, ensuring that daily consumption patterns reflect coherent operational behavior rather than isolated hourly samples.

To reach this goal, K-Nearest Neighbors Regression (KNN) (KNN algorithm: Introduction to K-Nearest Neighbors) is used, which is a regression technique, that predicts the output for a new sample by averaging outputs of its K nearest neighbors in the training data. Inputs (features) and/or outputs (targets) are functions, not vectors. In addition, the functional distances (e.g., L^2 norm or FPCA-based distances) is used to compute closeness between curves. The used function is as follows:

$$\hat{y}(x) = \frac{1}{k} \sum_{i \in N_k(x)} y_i$$

Development of the proposed scenario generation tool consists of several sequential steps, as illustrated in Figure 2. SESST and its components: 1. Scenario generation tool, 2. Grid assessment module. The first stage involves data preprocessing, a multi-step process that is described in detail in Figure 3. Workflow of the scenario generation tool. due to its complexity and importance. Once preprocessed, the data is provided to a KNN regression model, which predicts complete daily demand curves for the test set by identifying the most similar patterns from the training set, based on functional distance metrics. In the current implementation, the default functional distance metric provided by the scikit-fda KNN

regressor is used, together with distance-based weighting of neighboring observations. The KNN model uses K=25 nearest neighbors. The value of K is an adjustable hyperparameter and can be adapted depending on the problem setting and characteristics of the available data. The model generates demand scenarios at hourly resolution for a single 24-hour period. Each scenario represents a full daily load profile, capturing intra-day dynamics such as ramping behavior and peak formation. The approach focuses on variability within a day rather than modelling chronological dependencies between consecutive days. Subsequently, 150 representative scenarios are generated through Fuzzy C-Means clustering of the predicted functional demand curves.

Following the prediction step, the generated demand curves are grouped using Fuzzy C-Means clustering (Pattern Recognition with Fuzzy Objective Function Algorithms | SpringerLink). This enables the identification of representative load patterns while accounting for variability and uncertainty across scenarios. In the final step, the resulting demand scenarios are exported as CSV files. The output profiles are structured as standardized 24-hour time series, enabling direct integration into the grid assessment module of the SESST. In addition, the generated scenarios can be used in other grid-related analyses, such as load flow simulations, congestion studies, and long-term planning evaluations, making the tool applicable beyond the immediate scope of this project. Furthermore, the scenario generation tool is modular and transferable to other case studies or network areas. To ensure accuracy, the input data, such as demand history, weather variables, prices, and scenario assumptions, must be adapted to the specific characteristics of the new study area.

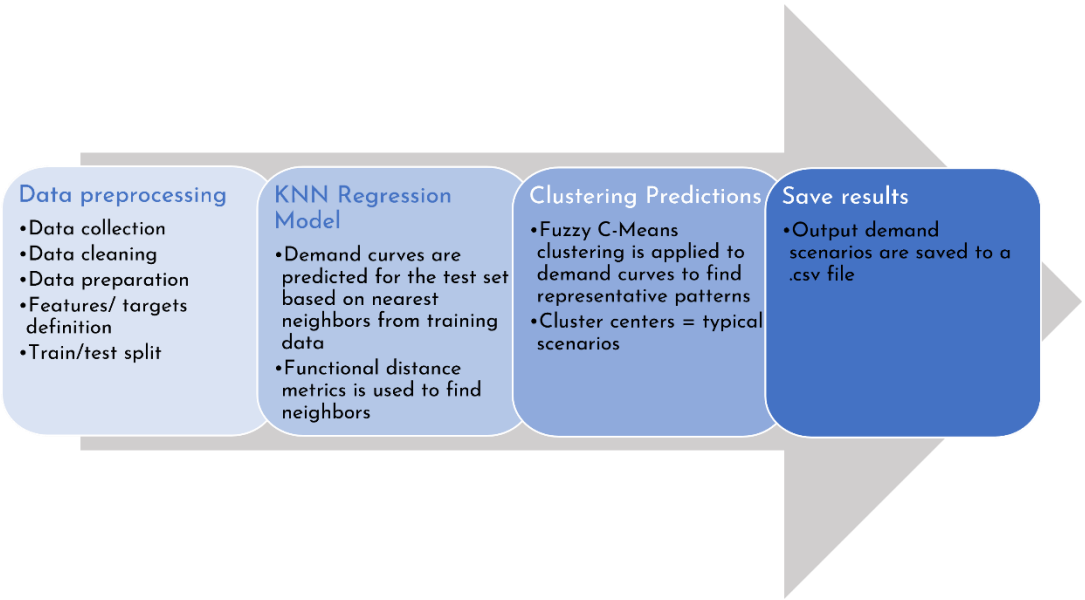


Figure 3. Workflow of the scenario generation tool.

The raw data provided by the industry partners often contains a considerable amount of information, covering multiple aspects of electrical system analysis, including operational measurements, asset characteristics, reliability indicators, and network configuration information. Although this richness is valuable, not all variables are directly relevant to demand scenario generation and grid operation modeling. In addition, differences in format, time resolution, and naming conventions require harmonization before the data can be used within the modeling framework. Similarly, data obtained from publicly available sources may require alignment to ensure compatibility with the analysis requirements. Consequently, a

structured preprocessing phase is necessary to filter relevant parameters, standardize formats, and transform heterogeneous raw inputs into a consistent, analysis-ready dataset suitable for the subsequent modeling stages.

It should be noted that the specific preprocessing steps described in this section are tailored to the characteristics and objectives of this demonstration project. Different datasets or applications may require adapted preprocessing procedures depending on their structure, content, and intended use.

Accordingly, the data preprocessing phase of the tool consists of the following sequential sub-steps, as also shown in Figure 4:

1. **Data collection:** Historical datasets were gathered for electricity demand, day-ahead electricity prices, and weather conditions covering the period from 2017 to 2022. The electricity demand data were obtained from real industrial measurements shared by the Port of Sines with TU Delft, providing a realistic representation of consumption behavior in an industrial setting. Complementary data on renewable generation potential (solar and wind profiles) and day-ahead electricity prices and regional weather information were retrieved from online websites (Renewables.ninja, Transparency Platform). Although access to measured industrial demand data depends on data ownership and sharing agreements, the proposed tool can also operate using standardized open-source datasets, ensuring applicability even when proprietary measurements are unavailable.
2. **Data cleaning:** The collected data had to be cleaned to ensure consistency and usability. This included renaming columns for clarity, removing redundant or irrelevant fields, handling missing values, and aligning timestamps across different datasets. Additionally, all datasets were resampled to an hourly resolution to ensure a common temporal granularity.
3. **Data preparation:** After cleaning, the data underwent a preparation stage which included seasonal segmentation (e.g., splitting data by month or season), random sampling to ensure diversity and representativeness, and transformation of the time series data into a functional data format. This transformation facilitates the use of FDA techniques later in the modeling process.
4. **Features and target definition:** In this step, the features (independent variables), including weather and price data, were clearly defined and aligned with the targets (dependent variable), which is the hourly energy demand.
5. **Train-test splitting:** Finally, for each season or selected month, the dataset was divided into training and testing subsets. For each season or selected month, the dataset was divided using a time-based (chronological) split, where data from selected months were used for training and non-overlapping months for testing. Each day was treated as one sample, and only days with complete 24-hour observations were retained, resulting in sets of daily functional profiles with clear temporal separation. This step is essential to evaluate the generalizability and performance of the scenario generation model. Model performance was evaluated using the Mean Absolute Error (MAE) between observed and predicted daily profiles from the KNN regression model. Additionally, the generated scenarios (Fuzzy C-Means cluster centers) were assessed based on their ability to capture variability in the predicted functional space.

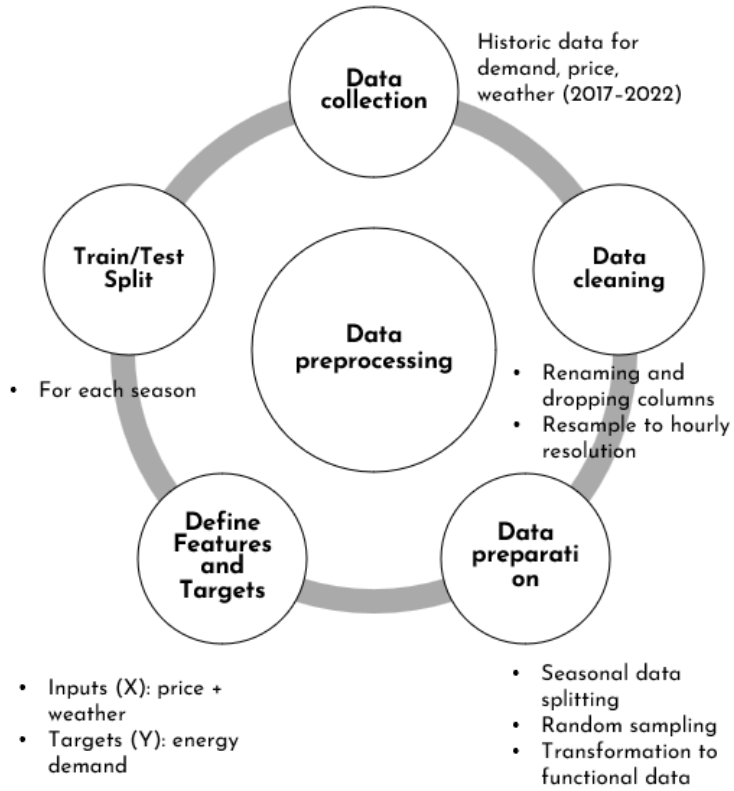


Figure 4. Data pre-processing steps.

2.3.2 Inputs/Outputs

The scenario generation model requires several key inputs to function effectively, including:

- The selected month for which demand scenarios are to be generated, enabling seasonal differentiation in the results.
- The number of scenarios to be generated, allowing users to control the breadth of uncertainty representation.
- Historical datasets, which are essential for training the model including energy demand profiles, day-ahead electricity prices, and weather data (e.g., temperature, wind speed, solar irradiance).

The core of the model is a functional KNN regression approach. Unlike traditional point-wise KNN, this method operates on entire daily demand profiles, treating them as functional data. For each test instance (a day in the selected month), the model identifies the most similar historical days, based on both weather and price conditions, and uses their demand profiles to predict new scenarios.

As output, the model generates the specified number of full daily energy demand curves for the chosen month, each representing a plausible scenario under given seasonal and market conditions. This entire process is illustrated in Figure 5, providing a visual overview of the model and its inputs and outputs.

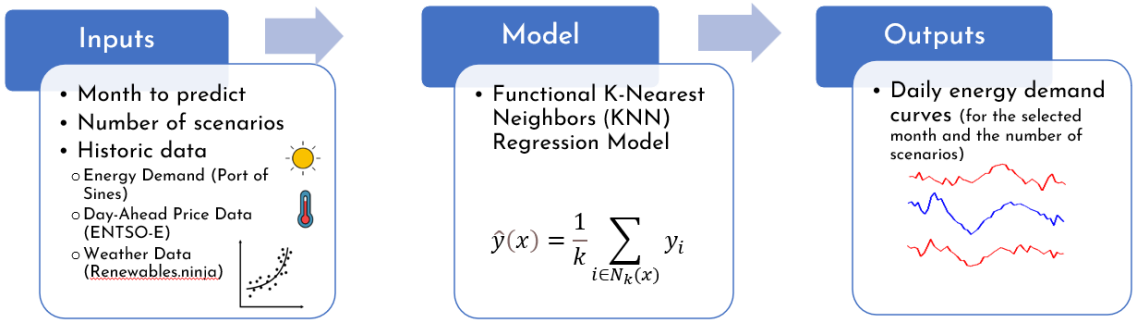


Figure 5. Scenario generation tool and its inputs/outputs.

2.4 Grid assessment module

2.4.1 Description of the model

The grid assessment module is a Python-based analytical framework designed to evaluate the performance and future adaptability of an electrical distribution network. The module consists of four main components: (i) base case analysis, (ii) assessment of future expansion plans, (iii) MC simulations, and (iv) KPI calculations.

1) **Base case analysis:** This stage involves a detailed assessment of the existing electrical infrastructure of the case study. It includes identifying the network topology, component characteristics (such as lines, transformers, loads, and distributed energy resources), and their interconnections. A single-line diagram is developed to visualize the system structure. The complete electrical network model is then implemented and simulated using a PF analysis representing the present-day operating state of the system. Specifically, the base case considers the current grid configuration without any planned network reinforcements or expansions, the existing installed capacities of loads and DERs, and measured or nominal operating power levels representative of typical present-day conditions. Future electrification pathways, demand growth projections, and energy transition scenarios are intentionally excluded at this stage. The PF analysis therefore evaluates the operational performance of the network as it currently exists, including voltage profiles, line loadings, and potential bottlenecks.
2) **Analysis of future expansion plans:** In this part, the potential future developments of the grid are estimated based on the expansion plans provided by the case study. This includes analyzing planned infrastructure upgrades, anticipated load growth, integration of renewable energy sources, and new connection points. The goal is to assess how these changes may affect the grid's operation in future scenarios.
3) **MC simulations:** To account for the uncertainty associated with load demand variations, a MC simulation framework is developed. This part of the module performs multiple PF analyses under a wide range of randomly generated load demand scenarios. The load profiles are sampled from predefined probability distributions that reflect realistic variations in consumer behavior and demand patterns. By repeatedly running the PF analysis for these sampled scenarios, the MC framework provides a probabilistic assessment of the grid's performance, enabling the identification of voltage deviations, line overloads, and potential congestion points under different demand conditions.
4) **KPI calculations:** The final step focuses on calculating KPIs that quantify the overall grid performance from both general sustainability and technical operational perspectives. The KPI framework includes general indicators commonly used in energy system planning, capturing economic, environmental, and social performance aspects, as well as technical indicators widely adopted in electrical power system analysis. The technical KPIs evaluate voltage profiles, current magnitudes, line utilization, and

congestion severity to assess infrastructure performance and operational reliability. These indicators are not specific to port systems but are applicable to a wide range of electrical networks. Based on the simulation outcomes, the module identifies critical network segments prone to congestion and evaluates the potential for deploying flexibility services and renewable energy integration to enhance the grid's operational efficiency across different scenarios.

2.4.2 Inputs/Outputs

Figure 6 presents a comprehensive overview of the grid assessment module, outlining its key components, inputs, and outputs. The overall workflow integrates deterministic and probabilistic analyses to evaluate the grid's operational performance under current and future conditions.

The process begins by defining the grid configuration and specifying the electrical components that form the network topology. This includes transformer ratings, line impedances, distributed generation specifications, and planned future network extensions. The main inputs to the base case analysis are the grid configuration and component data, while the outputs, after performing AC PF simulations, include steady-state voltage and current profiles, as well as line losses for the existing grid configuration. Subsequently, the same analysis is repeated, considering the future extension plans, creating an extended base case. The inputs for this second step include the future extension plans of the grid, and the updated grid configuration incorporating the future extensions, while the outputs are the corresponding PF results under the extended network conditions. These two stages assess the network's capability and limitations under both present and near-future conditions.

The next stage of the workflow involves MC simulations, which provide a probabilistic assessment of grid performance under a wide range of operating conditions. The inputs to this stage include historical RES generation profiles, electricity prices, the grid configuration from earlier steps, and synthetically generated load demand time-series data representing different demand scenarios. For each realization $i \in \{1,2,\cdots N\}$, a distinct power flow problem is solved: $f(V_i, \theta_i, P_i, Q_i) = 0$, where P_i, Q_i represent the active and reactive power injections for the i^{th} scenario, and V_i, θ_i denote the corresponding voltage magnitudes and angles obtained from the PF solution. The outputs of this MC stage are scenario-specific results, including voltage and current magnitude profiles, power losses, and other system specifications for each realization. By repeating this process across N randomly generated scenarios, the MC framework captures the statistical spread of operating conditions, quantifying how voltage levels, line currents, and power losses vary in case of each realization of load demand scenarios.

According to the obtained outcomes, the relevant KPIs are then calculated, including the number of assets operating under congestion and their congestion levels, renewable energy curtailment (%), power losses (kW), and the ratio of peak power and self-consumption (%). The inputs for this final stage are the aggregated results from all MC simulations, while the outputs are the computed KPIs that summarize the grid's overall performance under various realized scenarios. These indicators provide a comprehensive understanding of the grid's robustness and flexibility, revealing how often and under what conditions the system may experience stress or inefficiencies. This insight helps evaluate the network's readiness to accommodate additional load or generation and informs strategic decisions for grid reinforcement and renewable integration.

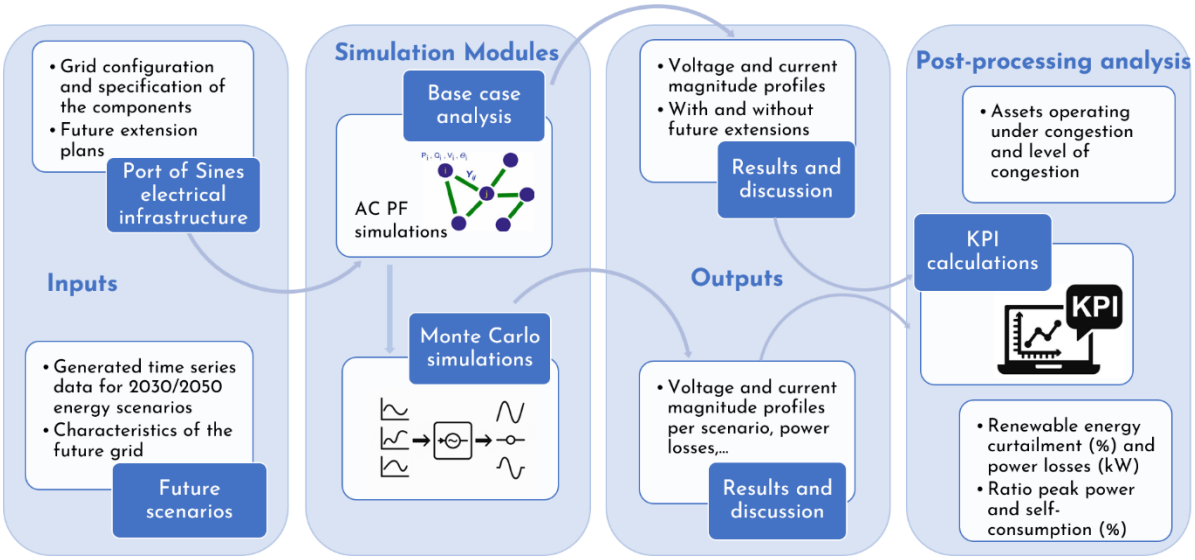


Figure 6. Grid assessment module and its inputs/outputs.

2.5 Summary of tool capabilities, implementation, and accessibility

Application context, scalability, and objective

The tool is designed to support long-term energy planning and grid operation studies by generating realistic future demand scenarios and assessing network performance under uncertainty. Although demonstrated using a port case study, the framework is applicable to different electrical grid, including urban networks, industrial zones, logistics hubs, and regional power systems. Scalability extends beyond grid size due to the tool's modular architecture and function-based implementation. It is adaptable to different network scales, grid topologies, component specifications, and operational characteristics. However, application to a new case requires updating the network structure data and operational datasets according to the specific case study.

The framework supports both existing grid configurations and future grid developments, enabling evaluation of present operating conditions as well as planned infrastructure expansions, electrification pathways, and renewable energy integration scenarios.

Programming language and main libraries used

The tool is implemented entirely in Python, leveraging key libraries such as pandas (https://pandas.pydata.org/) for data handling, NumPy (https://numpy.org/) and SciPy (https://scipy.org/) for numerical computations, scikit-learn (https://scikit-learn.org/) for KNN regression modeling, scikit-fuzzy (skfuzzy) (https://pythonhosted.org/scikit-fuzzy/) for Fuzzy C-Means clustering, and pandapower (https://www.pandapower.org/) for PF simulations. Additional libraries like matplotlib (https://matplotlib.org/) and seaborn (https://seaborn.pydata.org/) support visualization and result analysis.

Accessibility for users

The tool is maintained in a public GitHub repository (neda-vahabzad/Demo2_MAGPIE_project_simulations_code), to ensure transparency, reproducibility, and accessibility. Due to data confidentiality agreements, the case study datasets used in this work cannot be publicly shared. Therefore, the publicly available version provides the complete modeling framework without proprietary data, allowing external users to apply the tool using their own network and operational datasets. The full version, including project-specific data, is accessible only to MAGPIE project collaborators upon request via

MAGPIE SharePoint to enable coordinated development and application within the project. The tool is intended to support stakeholders involved in energy system planning and grid operation, including distribution system operators, infrastructure planners, industrial energy managers, policymakers, and researchers. Beyond open-source access to the framework, active dissemination is foreseen through collaboration with industry stakeholders, integration into planning workflows, and the development of user-oriented documentation and training materials to facilitate practical adoption.

3. Case study-Port of Sines

3.1 Overview

The case study considered in this work is the Port of Sines (apsinesalgarve.pt/en/ports/port-of-sines/), located in Portugal. Figure 7 presents the geographical map of the port. The electrical infrastructure of the Port of Sines comprises several substations and transformer stations distributed across its jurisdiction, ensuring the supply of medium- and low-voltage electricity throughout the area. The internal distribution grid is managed by APS (administration of the Port of Sines), which owns and operates the port's electrical infrastructure. This allows APS to plan, operate, and coordinate the integration of new energy assets within the port. Although the regulatory framework governing electricity distribution differs across EU Member States, many large European ports have similar governance structures in which the port authority is responsible for managing the internal electricity distribution network. Therefore, the Port of Sines provides a representative case study for ports with comparable governance and operational responsibilities, while acknowledging that the legal allocation of these responsibilities may vary between countries.

Historically, the port's electrical grid was supplied from the public network at 30 kV through three mixed overhead/underground lines. Each of these connections could deliver up to 10 MVA and was capable of operating independently to meet the port's total power demand. Currently, a new 60/30 kV substation with a maximum capacity of 63 MVA is under construction to connect the port to the 60 kV public grid via two redundant overhead lines. This substation was commissioned in 2026 and supplies the existing 30 kV network through two underground feeders, permanently replacing the former 30 kV inputs. Consequently, all analyses and evaluations in this study consider the 60/30 kV substation as the main supply point.

As illustrated in Figure 8, the port's electrical network operates across multiple voltage levels: a 30 kV system supplying the eastern zone, a 15 kV network serving the western area, and additional 6 kV and 6.6 kV networks dedicated to various customer loads and services.

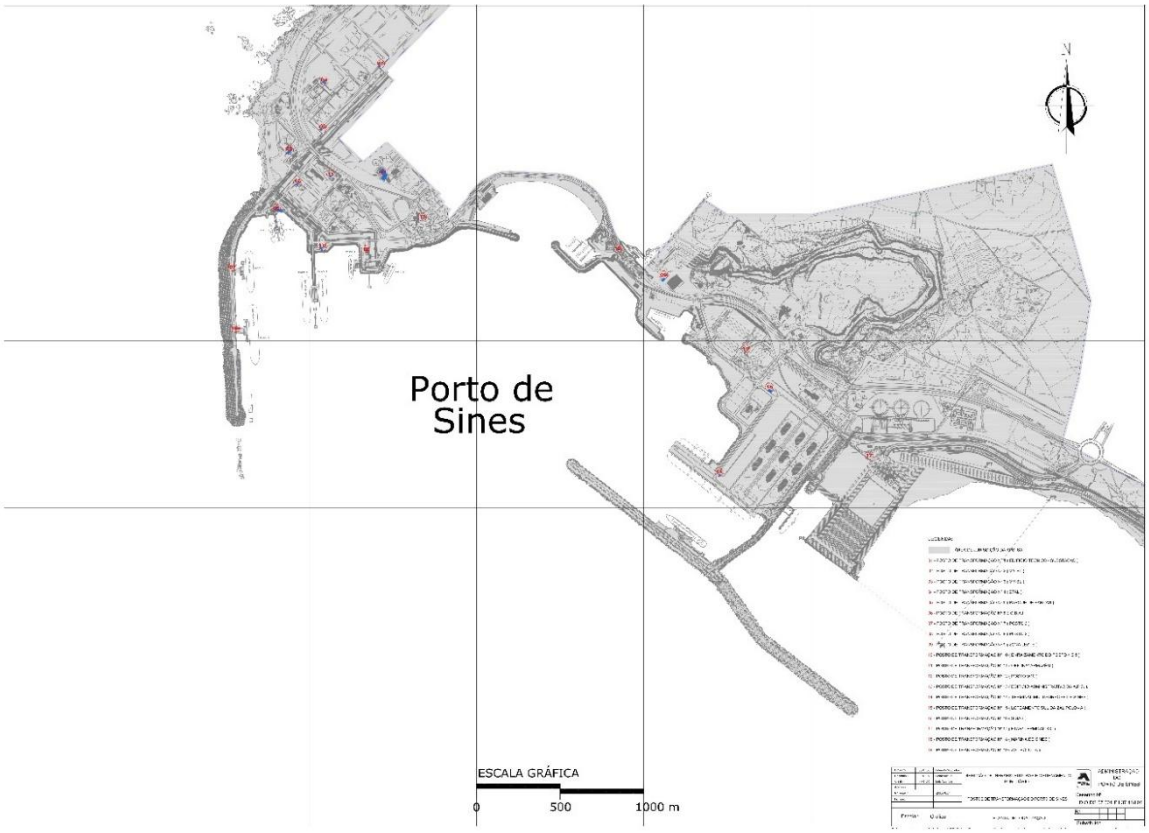


Figure 7. Geographical map of Port of Sines.

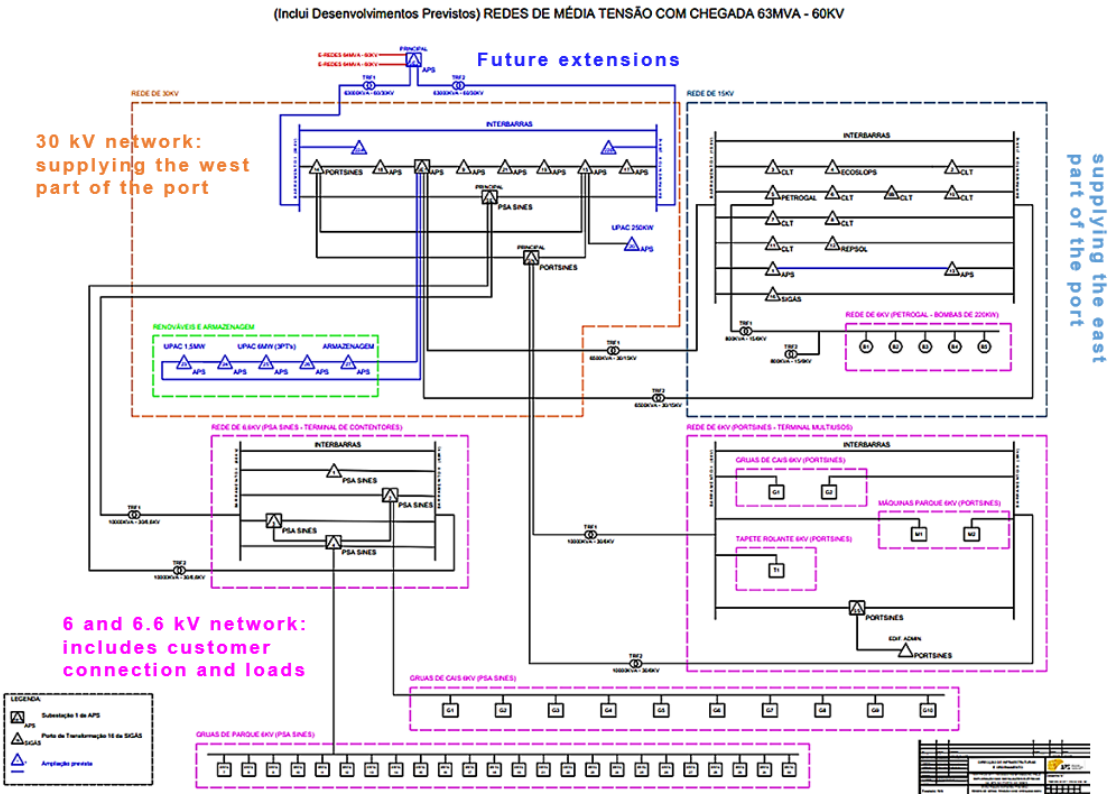


Figure 8. Port of Sines electrical infrastructure, and its different voltage levels.

30 kV network

The 30 kV network is designed to distribute electricity across the broader service area through a system of transformation stations located throughout the region, also supplying connected medium-voltage (MV) customers. This network configuration ensures high service reliability through a ring feeder arrangement, in which distribution lines form a closed loop that allows electricity to be supplied from multiple directions. In such a configuration, if a fault occurs on one section of the feeder, the affected part can be isolated while the remaining network continues to supply customers through an alternative path, as illustrated in the schematic diagram. A few transformation stations (including PT17, PT18, PT19, PT21) currently operate with radial feeders, where each feeder supplies loads through a single path from the substation without an alternative supply route. These stations are planned to be upgraded to ring configurations as part of the ongoing 60/30 kV substation development. The entire 30 kV network is implemented underground, using single-core cables arranged in a cloverleaf formation, where three phase conductors are positioned close together in a triangular configuration to reduce electromagnetic interference and improve thermal performance.

15 kV network

The 15 kV network is designed to distribute electricity within the industrial terminal area and to various service facilities managed by the APS authority. It operates through a network of transformation stations that supply multiple MV customers, namely CLT (PT2, PT3, PT6, PT6B, PT7, PT8, PT10, PT11), PETROGAL (PT5), REPSOL (PT12), SIGÁS (PT16), and ECOSLOPS (PT4), via a ring-fed configuration, ensuring high reliability and service continuity. The network primarily consists of exposed three-core cables installed along dedicated tracks or cable tunnels, with certain sections buried to accommodate crossings or pipelines. Ongoing modernization works include the replacement of some sections with single-core cables, while other parts remain in three-core configurations, depending on

operational management responsibilities between the APS Port Authority and industrial operators. While the main role of the 15 kV network is to supply electricity within the terminal area, it also serves a few external facilities, including PT1 (Technical Building and Fire Station) and PT13 (Administrative Building), through radial-feed transformation stations. These have been reconfigured to ring-feed connections as part of the 30/15 kV substation modernization project, which has already been completed.

6 and 6.6 kV networks

The port's 6 kV and 6.6 kV networks supply power to distinct terminals and facilities, each operating independently under its respective ownership. The 6.6 kV network, owned by PSA Sines, serves the container terminal, providing electricity to 10 quay cranes (gantry cranes) and 24 electrically powered rubber-tired gantry cranes (E-RTGs) for container handling operations. The 6 kV network at the multipurpose terminal, operated by PORTSINES, supplies power to quay cranes, stacking and retrieval machines, and a conveyor system connecting the quay to the storage area. Another 6 kV network, exclusively serving the bunkering facility owned by PETROGAL, powers five 220 kW pumps used for refueling vessels at the liquid bulk terminal.

This study focuses on the 30 kV network, with the 15 kV, 6 kV, and 6.6 kV systems considered as aggregated loads connected to it. Figure 9 presents a detailed single-line diagram of the 30 kV network, illustrating all buses, lines, transformers, switches, and generators with their technical specifications. Connection points to the lower-voltage networks are shown in green, while planned future extensions are highlighted in red.

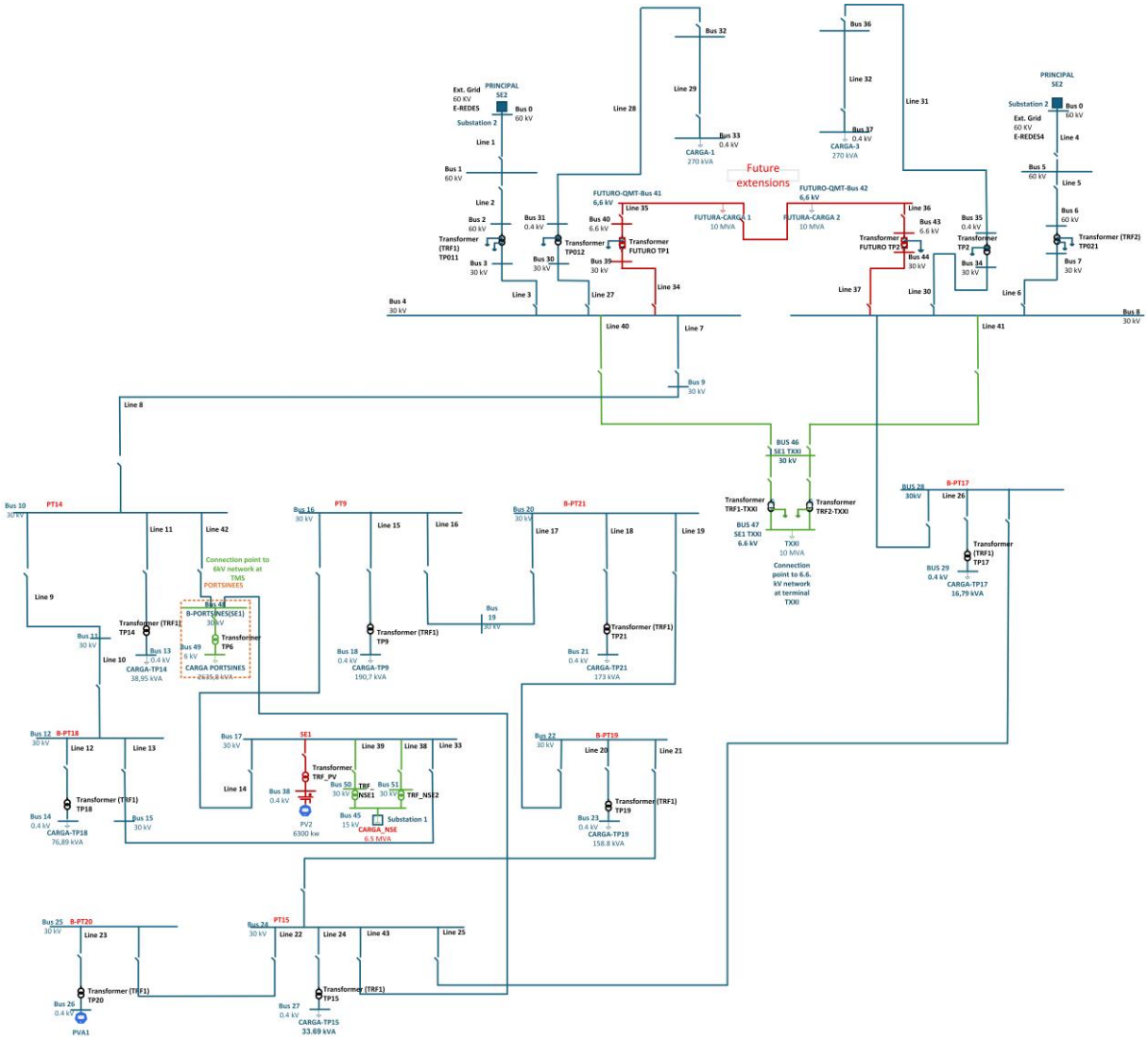


Figure 9. Single-line diagram of the 30 kV network. Connections to other grids are shown in green, while planned future extensions are highlighted in red.

3.2 Energy transition plans in Port of Sines

Objectives and goals

Aligned with the EU external energy policy, the Port of Sines aims to achieve 100% carbon neutrality by 2045. As part of this objective, the port is investing in grid upgrades, renewable energy integration, electric mobility, and electrification of vessels. Additional initiatives under consideration include energy storage, alternative fuels, and (OPS) solutions for shipping. In this study, the analysis focuses on the electricity infrastructure and the technologies and capacity expansions provided by the port stakeholders. The results therefore reflect the contribution of these elements to the port's energy transition, rather than a comprehensive representation of the full decarbonization pathway of all activities within the port area.

Renewable energy generation

The energy transition is essential, and clean energy planning requires a diversified energy mix. APS is exploring the integration of multiple RES, including solar (PV), wind, and wave energy, as it is illustrated in Figure 10 Investing in renewable energy generation within the

APS jurisdiction is a key priority. In 2023, there was no installed renewable capacity. The planned deployment includes a total of 6.3 MW of solar PV capacity, to be installed in two phases: Phase 1 (1.5 MW) and Phase 2 (4.8 MW). The PV installation is not yet operational and is scheduled to enter operation in September 2026.

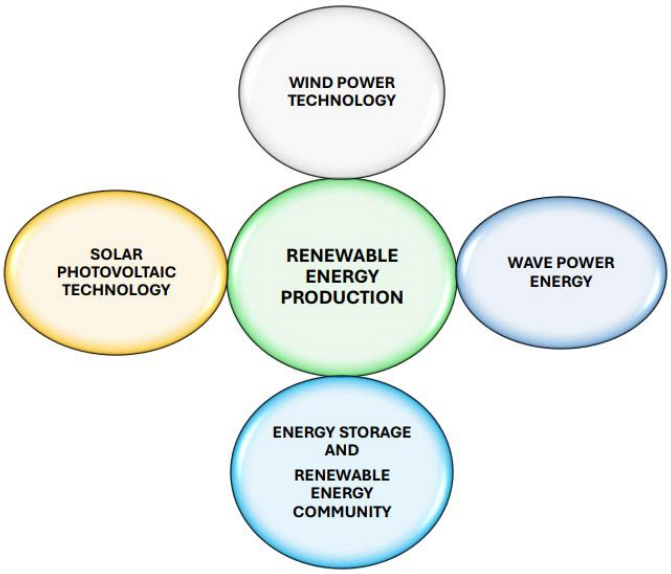


Figure 10. Renewable energy generation plans in Port of Sines.

Exploring the feasibility of installing a wind farm at the Port of Sines is underway to boost RES integration on-site. Additionally, wave energy potential is being evaluated through the NEXUS Agenda, which will deliver and test a small-scale wave energy converter. The NEXUS Agenda is expected to significantly contribute to the port's green transition goals by supporting the development of key innovations, including an energy management system, OPS solutions, wave energy conversion technologies, UAV-based PV systems, an environmental digital platform, and electric vessels.

Energy storage

The integration of storage technologies enables strategic planning of energy consumption by allowing control over when the produced energy is used, thereby minimizing surpluses. Various storage solutions are currently being evaluated based on available technologies, considering factors such as capacity, autonomy, and investment planning.

Power supply for ships (OPS)

OPS systems are planned to be installed across APS ports, including four systems at the container terminal in the Port of Sines and one at the cruise terminal in the Port of Portimão. Each OPS installation is designed with a rated power of 8 MVA, while the value of 10 GWh/year refers to the expected annual energy delivered by each system, rather than its instantaneous power capacity. The OPS systems are intended to serve vessels that are compatible with shore power and are berthed at the equipped terminals; therefore, they are not expected to supply all visiting vessels. The estimated annual energy demand is based on the current and projected vessel traffic forecasts provided by APS. Although five OPS systems will be installed across the APS ports, simultaneous operation of all systems at their rated power is not considered a normal operating condition, as their utilization depends on vessel arrivals and berth occupancy. Consequently, in the network studies, the OPS demand is represented using dedicated load profiles derived from the expected operational schedules and energy demand forecasts. These profiles were incorporated into the load profile generator to capture the future electrification of port operations. Overall, the OPS

installations are expected to meet approximately 40% of the ports' electricity needs by 2030, with overall electricity consumption projected to quadruple by then.

Electric mobility

APS has been actively investing in electric mobility by expanding its EV charging infrastructure and fleet. Charging stations have been installed at various APS facilities, including:

- A double tower charger (44kW/2×22kW) at both the APS Technical Building and Head Office
- Additional wall box chargers at the Head Office (one simple 22kW wallbox and two double wallbox chargers totaling 44kW/2×22kW)
- The Administrative Houses are equipped with three double wallbox chargers (22kW/2×11kW), and the Pilots' House has one double wallbox charger (22kW/2×11kW)
- In addition, APS operates a fleet of 13 electric vehicles, supporting the company's transition to sustainable transportation.

Electric boats and supply

As part of the NEXUS agenda, APS is advancing its commitment to sustainable maritime operations by developing 100% electric boats. This includes the construction of a new electric pilot boat, a new electric multi-task boat, and the retrofitting of the existing Porto Covo fuel-powered boat to become fully electric. To support these vessels, OPS systems will be implemented in two phases: initially, the charger/OPS system will be installed at the APS service port, and in the second phase, it will be relocated to the future cryogenic liquefied gas terminal.

Modernization and expansion of the electrical grid

A new 60/30kV substation, set to become operational this year and connected to the national high-voltage grid, will provide APS with increased power availability and enhance the stability of the port's electrical network. Alongside this development, APS is renewing its existing electrical grid infrastructure with a focus on implementing a centralized communication system across the entire network.

Energy management systems

The NEXUS Agenda and the EU-funded ELEXIA project are currently developing energy monitoring service (EMS) platforms that leverage the port's existing infrastructure and planned future developments. These platforms will enable real-time monitoring of energy consumption and generation, while also offering advanced functionalities for energy analytics, storage, and management.

Alternative fuels in the shipping industry

APS is actively cooperating with terminal operators to support the handling of alternative fuels, including ammonia, methanol, and biofuels. In parallel, a new cryogenic liquefied natural gas (LNG) terminal is under development to enable the supply of natural gas for ship bunkering and transshipment to other ports, further advancing the port's commitment to cleaner and more sustainable fuel solutions.

Renewable energy community

The constitution of a renewable energy community (REC) enables the valorization of renewable overproduction and allows the benefits of port renewable generation to be shared with surrounding REC members beyond the physical boundaries of the port through the public electricity grid.

Figure 11 presents an aerial view of the port map, highlighting the approximate locations of the planned developments described above.



Figure 11. Aerial view of the planned developments in the port.

Not all of the above-mentioned extension projects are currently in the implementation phase, and some lack finalized specifications or defined connection points within the grid. Wind and wave energy technologies are currently not included in APS's investment plans. This is primarily due to their relatively low Technology Readiness Level (TRL) for the intended applications, combined with their high investment costs and the associated technical and economic uncertainties. Nevertheless, APS is actively monitoring technological developments and evaluating the future potential of these renewable energy technologies as they become more mature and economically viable. To ensure an accurate representation of the ongoing modernization efforts, only the developments that have been completed or are nearing implementation are included in this analysis, including:

- ✓ 6.3 MW of PV capacity installed, comprising Phase 1 (1.5 MW) and Phase 2 (4.8 MW).
- ✓ Installation of an ESS adjacent to the PV units.
- ✓ Grid modernization, including the construction of a new 60/30 kV substation connected to the national grid and the implementation of a centralized communication system across the port's electrical network.
- ✓ Connection of two new lines supplying power to two 10 MVA loads.

4. Results

4.1 Generated scenarios

Figure 12 illustrates the load demand scenarios generated by the scenario generation tool for four representative months, each corresponding to a different quarter of the year. The tool stochastically produces hourly resolutions for daily demand scenarios, by selecting the target month and the number of scenarios (2–150), using probabilistic sampling based on historical load data and seasonal consumption patterns. The resulting profiles capture typical daily trends as well as uncertainties driven by user behavior, temperature, and operational schedules. As shown, each subplot represents a month: February (Q1), May (Q2), August (Q3), and November (Q4). Each quarter exhibits distinct seasonal characteristics: winter months (Q1) show generally higher demand, reflecting increased heating requirements, while summer months (Q3) exhibit flatter daytime profiles with lower overall consumption due to reduced heating and moderate cooling needs. Transitional months (Q2 and Q4) present more variable demand patterns with noticeable peaks during working hours.

Increasing the number of generated scenarios enhances the representation of uncertainty within each quarter, leading to wider percentile bands (10th–90th percentile) that better capture the potential range of operating conditions. This allows system planners and analysts to assess grid flexibility and robustness under varying demand realizations. The mean and median profiles (solid and dashed lines, respectively) represent the central tendency of the simulated demand, providing valuable reference profiles for use in planning, forecasting, and probabilistic PF studies.

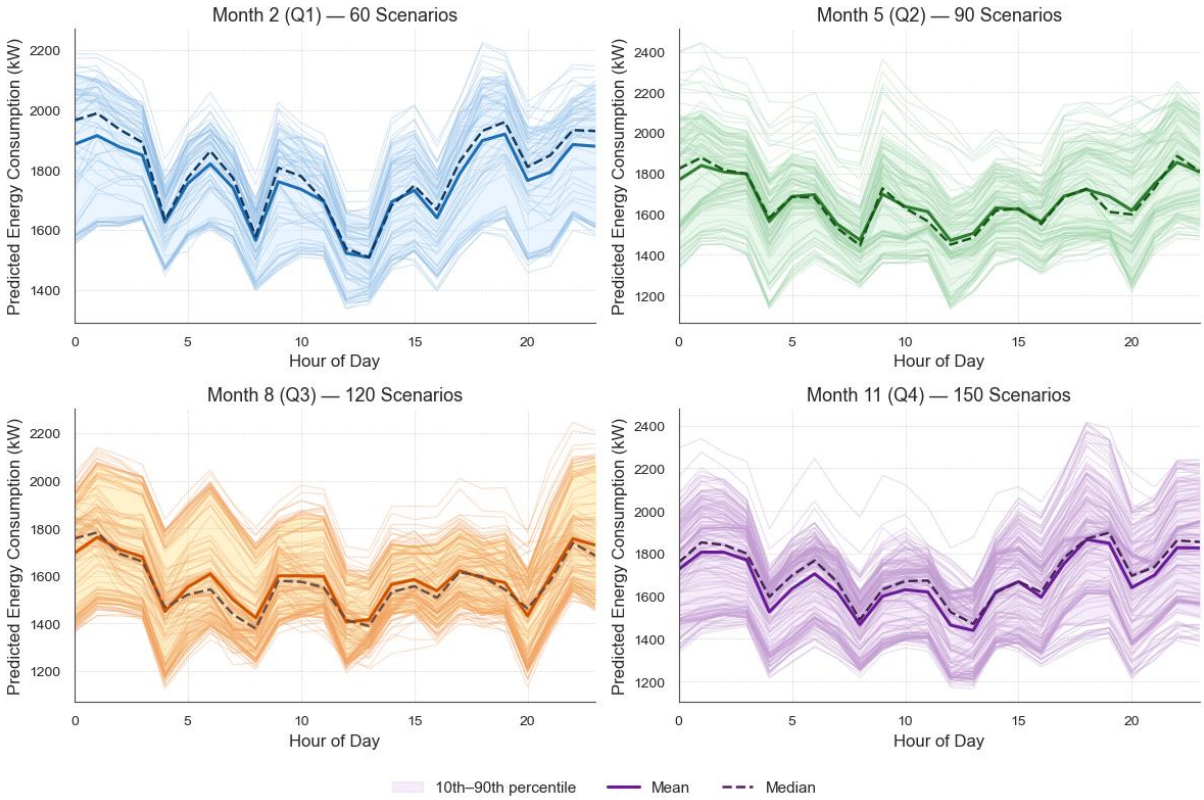


Figure 12. Seasonal load demand profiles generated for four representative months with different numbers of scenarios.

4.2 Base case analysis

The base case analysis involves evaluating the operation of the 30 kV electrical network of the Port of Sines across different configurations, using real network data and component specifications provided by the Port of Sines. The objective of this analysis is to assess the steady-state operational performance of the grid under both current and planned near-future conditions, focusing on voltage and line loading profiles, transformer utilization, and power losses. To capture the technical impact of the surrounding networks (highlighted in green in Figure 8 and the nearly completed extensions (marked by red), four operating modes are examined through PF simulations:

- **Mode 1- Isolated operation:** The existing 30 kV grid operates in isolated mode, with all interconnection switches to neighboring networks (15 kV, 6 kV, and 6.6 kV) open. The system includes the newly inaugurated 64 MVA, 60 kV substation but excludes any planned extensions.
- **Mode 2- Interconnected operation:** The same network configuration as Mode 1 operating in connected mode to other networks (15, 6 and 6.6 kV networks)
- **Mode 3- Isolated operation with planned extensions:** The existing 30 kV network operates in disconnected mode, with the interconnection switches open. Planned extensions are included, specifically, the 6.3 MW PV system, the energy storage unit, and two additional 10 MVA load points representing the new terminals on the western side of the Port, including the associated Onshore Power Supply (OPS) demand.

- **Mode 4: Interconnected operation with planned extensions:** The configuration from Mode 3 operates in the connected mode to the adjacent 15 kV, 6 kV, and 6.6 kV systems.

Figure 13 illustrates the statistical distribution of bus voltage magnitudes and line loading levels obtained from the PF simulations for the 30 kV network under the four operating modes. Line loading values are expressed as the percentage of the actual current relative to the maximum allowable current of each line. The comparison across modes highlights how network interconnection and planned system extensions influence both voltage performance and loading stress throughout the network. Figure 14 complements this distribution-based view with detailed bus-by-bus and line-by-line profiles, illustrating how voltages and line loadings evolve spatially across the entire network under each operating mode.

The observed differences across operating modes can be directly related to the underlying demand and generation levels summarized in Table 6. In particular, the significant increase in total load demand from Mode 1 (1.16 MW) to Mode 4 (38.34 MW), along with higher levels of local generation and self-consumption, explains the progressive increase in voltage variability and line loading across the network.

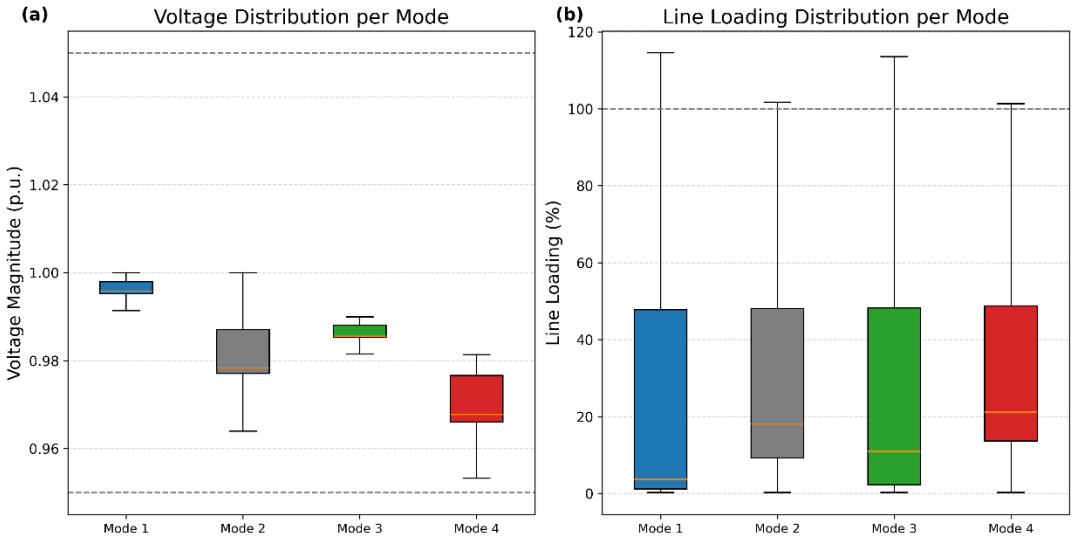


Figure 13. Statistical distribution of (a) bus voltage magnitudes and (b) line loading levels across the 30 kV network under the four operating modes.

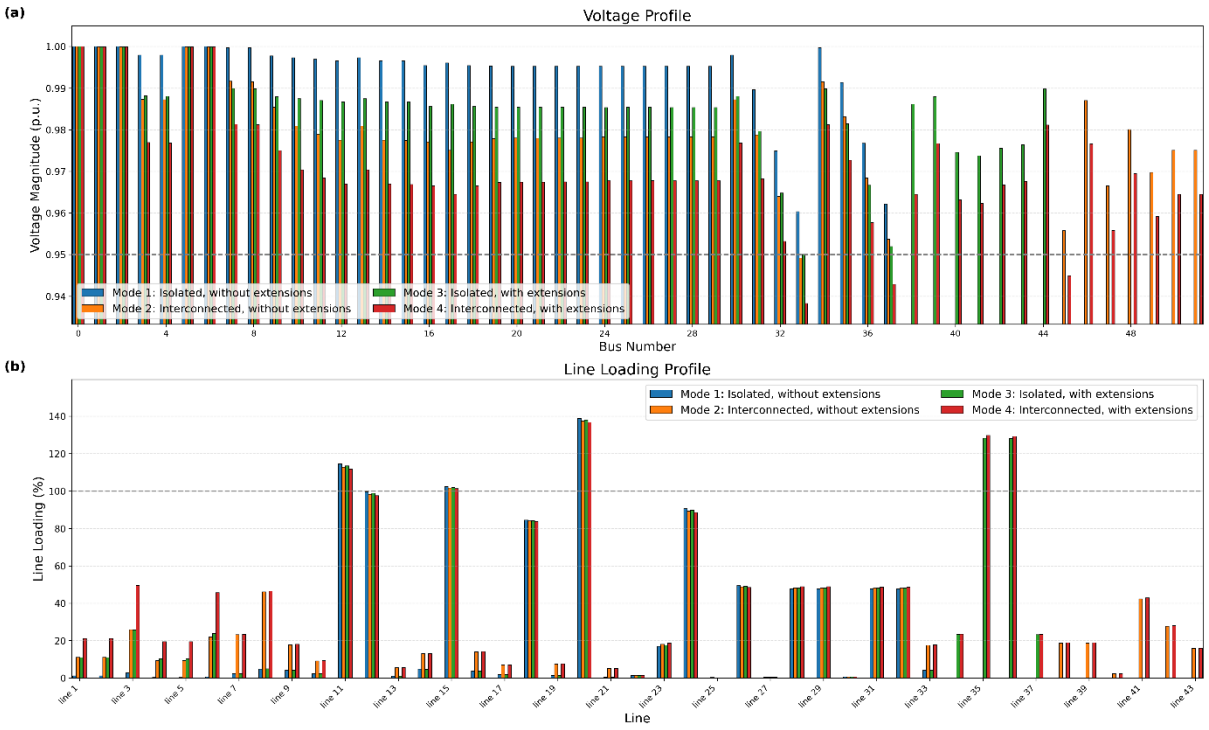


Figure 14. (a) Bus voltage magnitudes and (b) line loading levels for each bus and line under the four operating modes of the 30 kV network.

Voltage profile

Figure 13(a) shows that the distribution of bus voltages evolves across the operating modes as the system moves from Mode 1 to Mode 4. Mode 1 exhibits a tight cluster around 1.0 p.u., indicating stable and uniform voltages across the network under isolated operation without extensions. In Mode 2, the spread of the distribution increases and the median voltage shifts downward, reflecting the additional variability introduced by interconnection with neighboring voltage levels, and the higher load levels brought into the system through this interconnection.

Modes 3, however, shows a relatively concentrated distribution with a slight improvement compared to Mode 2, indicating that the integration of PV generation provides local voltage support and partially compensates for voltage drops. Mode 4 displays the widest dispersion and the lowest median voltage, indicating that the combination of interconnection, increased demand, and system extensions introduces the strongest variability and deviation from nominal conditions due to the presence of large additional loads connected to the network. This behavior is consistent with the increasing demand levels across the modes (Table 6), where higher loading conditions lead to larger voltage drops and increased dispersion.

These statistical trends are confirmed by the detailed voltage profiles in Figure 14(a). In Mode 1, the system remains well regulated, with only modest drops at heavily loaded buses 33 and 37, which are connected to the major load points CARGA-1 and CARGA-3. This behavior is expected since these loads represent the highest demand in the base grid configuration. Overall, the voltage levels remain well within the acceptable range of (0.95, 1.05) p.u., consistent with standard distribution network operational limits, indicating a balanced load distribution and sufficient reactive power support under the existing operating conditions. Mode 2 shows more pronounced reductions at downstream buses due to increased power exchange with external networks yet still maintains voltages within acceptable limits. Mode 3, which includes the planned extensions under isolated operation, demonstrates the

influence of both added loads locally connected PV generation in the 30 kV network. The new demand at buses 41 and 42 deepens local voltage drops, while the PV unit at bus 38 raises voltages in its vicinity. Mode 4 exhibits the most critical behavior, including under-voltages below 0.95 p.u. at buses 33 and 37 and localized over-voltages near buses closest to the external grid (including buses 3, 4, 7, and 8). While all modes remain within broader planning limits (0.9, 1.1) p.u., buses 33, 37, and 45 become increasingly sensitive as the system grows, indicating the need for voltage support solutions in case of future developments.

Line loading (%)

Figure 13(b) reveals a steady increase in both median loading and variability across the four operating modes. In Mode 1, most lines carry very low current, resulting in a narrow distribution with a median below 20%. Mode 2 introduces a noticeable upward shift, with higher median loading and a wider spread due to increased power transfers following interconnection. Modes 3 and 4 show the broadest distributions, with Mode 4 reaching the highest upper whiskers. This progression indicates that the combination of increased load demand, PV generation, and network interconnection leads to higher current flows, causing several lines to operate closer to their thermal loading limits. This trend is consistent with the substantial increase in total load demand and power flows reported in Table 6, which naturally results in higher line current magnitudes and increased utilization of network capacity.

According to Figure 14(b), in Mode 1, most lines operate at light loading, but a few, particularly Lines 11, 12, and 20, already exceed their thermal limits, revealing inherent bottlenecks in the existing network. As the system transitions to Modes 2, 3, and 4, loading remains critical on these same feeders, while additional stress appears on upstream lines close to the external grid, including Lines 1, 3, 7, and 9, which must carry higher currents due to increased power transfer. By considering the extensions, Lines 24, 35, and 36 also become significantly more loaded, especially under interconnected conditions. Mode 4 shows the highest loading levels overall, with Lines 35 and 36, linked to the new 10 MVA load additions, exhibiting the most severe overloads. Overall, while most line remain within safe loading limits in the base configuration, a small set of feeders,11, 12, 20, 24, 35, and 36, experience substantial loading increases as the network becomes interconnected and extended. This marks them as priority candidates for reinforcement and further considerations in case of future developments.

Transformer utilization (%)

Fout! Verwijzingsbron niet gevonden. indicates that most transformers in the 30 kV distribution network operate within a moderate loading range of approximately 40–70%, with noticeable variations across the four operational modes. In the isolated configuration without extensions (Mode 1), the two transformers directly connected to the external grid, TP011 and TP021, exhibit notably lower utilization levels (around 2% and 0.5%, respectively). This behavior is primarily due to the low overall load demand in the isolated mode and the fact that these transformers have a significantly higher rated capacity (63 MVA) than other units, which results in lower utilization ratios under typical operating conditions. Similarly, the TRF_PV transformer also shows a relatively low loading level, indicating that in the current operational configuration, the available PV generation capacity is not fully utilized under the current operational configuration. This suggests that a portion of the local renewable generation potential remains unused, leading to increased dependence on power imported from the external grid. Consequently, the system may experience reduced renewable energy penetration and potentially higher operational costs and emissions associated with external energy supply. Under an optimized operational strategy, where priority is given to local renewable generation, this transformer could operate at a higher loading level, thereby improving renewable energy integration and reducing power imports from the external grid.

In contrast, transformers such as TP17, TP18, TP20, and TP15 reach the highest utilization levels (approximately 64.5%) in Mode 1, reflecting their greater role in meeting local demand. As the system transitions to connected and/or extended configurations (Modes 2–4), transformer loading becomes more balanced, with moderate increases observed for the high-capacity and grid-connected transformers. The maximum loading across all configurations remains around 63–64% (for TP18 and TP20), confirming that the network operates efficiently without overburdening any transformer. Additionally, TP011 and TP021 exhibit the largest relative increases in utilization, up to 16–33 percentage by making the network interconnected and extended. Overall, all transformers operate well below their rated capacities, confirming that transformer overloading is not a concern under current or near-future configurations, while highlighting opportunities for further operational optimization and improved renewable energy prioritization in future network management strategies.

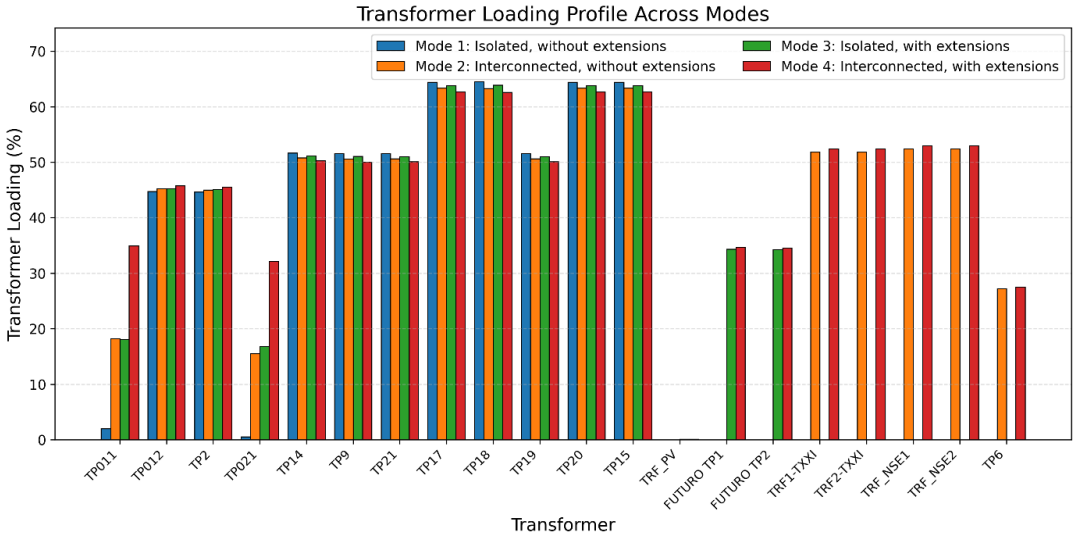


Figure 15. Comparison of transformer utilization (%) for the four operating modes of the Port of Sines 30 kV network.

Active power losses (kW)

Fout! Verwijzingsbron niet gevonden. in Figure 16 shows that losses remain generally low throughout the network, with only a few lines exhibiting significant magnitudes. In Mode 1, losses are minimal across nearly all lines, reflecting limited power transfer and low overall network loading. When the system transitions to Mode 2, a few lines, particularly Line 8, which connects Bus 9 (a central bus linking multiple feeders) to PT14, a key interconnection point, and Line 41, which connects Bus 8 (a central bus linking multiple feeders) to the 6.6 kV network, exhibit a marked increase in losses, reaching peaks of approximately 35–40 kW. These lines can therefore be identified as critical power transfer corridors. The addition of network extensions (Modes 3 and 4) introduces moderate additional losses on several feeders, particularly in the downstream sections of the newly connected areas. However, total network losses remain within acceptable operational limits across all configurations, with the most noticeable peaks occurring at the aforementioned lines, especially in Mode 4. This confirms that while network interconnection and extensions enhance operational flexibility and do not induce excessive losses, attention should be given to these high-loss corridors in future planning.

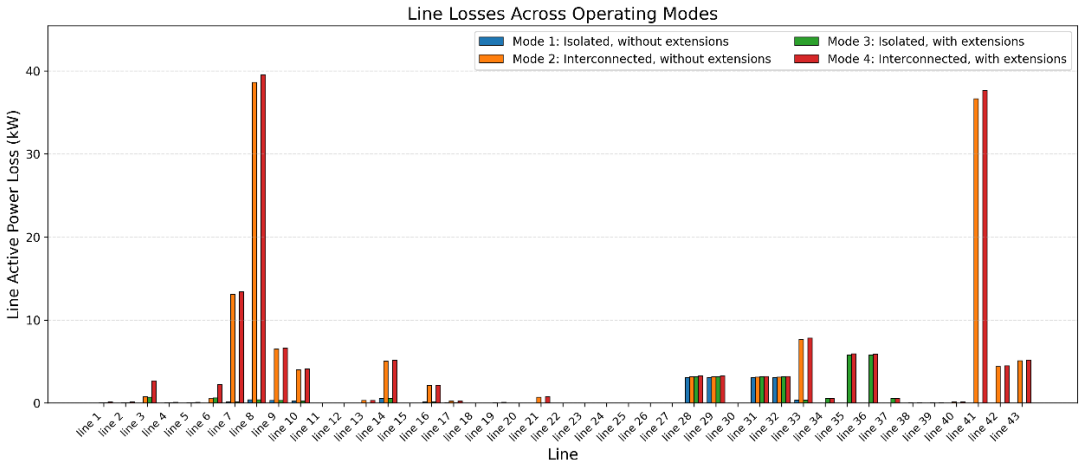


Figure 16. Comparison of line active power losses (kW) across the four operating modes of the Port of Sines 30 kV network.

4.3 MC simulations

The operational performance of the grid under future conditions is evaluated by conducting multiple PF analyses for a range of generated scenarios in each quarter of the year using MC simulation. Since the objective is to assess future operating conditions, the analysis accounts for projected load growth, the anticipated grid configuration including interconnections with other networks within the Port of Sines, and planned network extensions, as described in operation Mode 4 (Section 4.2).

Bus voltage and line loading

Figure 17 presents the hourly variation of bus voltages (left) and maximum line loadings (right) for all four generated quarterly scenario sets (Q1–Q4), as shown in Section 4.1. The reported values are obtained considering all buses and all lines of the studied 30 kV network. For each hour, the curves represent the median values across all Monte Carlo (MC) simulations, while the shaded regions indicate the minimum–maximum envelopes, capturing the variability among scenarios within each quarter. The median bus voltage remains highly stable throughout the day and across all quarters, typically within the range of 0.97–0.98 p.u. In power system operation, voltage magnitudes within 0.95–1.05 p.u. are generally considered acceptable operating limits. The results therefore indicate that the network can maintain adequate voltage regulation under most simulated operating conditions, even considering future load growth and the expanded grid configuration.

However, the lower bound of the Min–Max envelope occasionally decreases to approximately 0.94 p.u. during a limited number of time periods, revealing scenario-specific under-voltage events. These deviations suggest that certain combinations of high loading and unfavorable operating conditions may locally stress the network. For the proposed planning and operational assessment tool, this result is important because it demonstrates the capability of the framework to identify not only average system behavior, but also extreme operating conditions that could require corrective actions, such as local voltage support, network reinforcement, or operational rescheduling. In the context of the Port of Sines, these findings indicate that the future expanded network is generally capable of operating within acceptable voltage limits, although some critical operating periods may require additional operational flexibility or infrastructure reinforcement to ensure secure operation under all scenarios.

The line loading results, however, show a very different pattern. All four quarters exhibit pronounced diurnal variations, with multiple peaks occurring around early morning (hour 1–3) and evening hours (around 18–22), periods typically associated with high demand. Notably, for most hours and across all quarters, the median line loading exceeds 100%, indicating that several lines are persistently overloaded under the future grid reinforcement and interconnection assumptions. The wide Min–Max envelope across all sets highlights considerable uncertainty, with certain scenarios experiencing extreme loading conditions exceeding 125%. Among the quarters, Q3 (summer) and Q4 (winter) generally show higher peak loadings, reflecting the impact of seasonal load demand and possible DER variations.

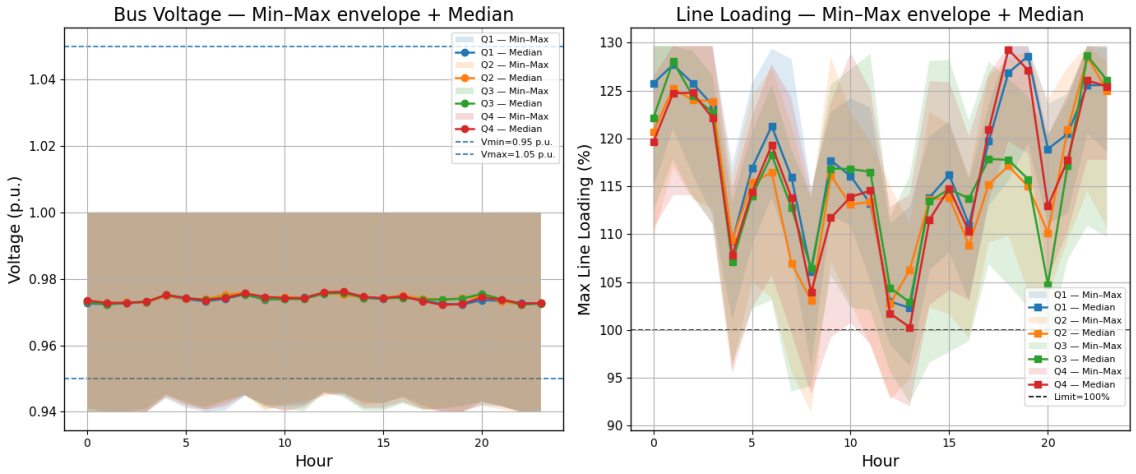


Figure 17. Hourly bus voltage (left) and maximum line loading (right) for all scenario sets (Q1–Q4), median trends and Min–Max envelopes relative to operational voltage (0.95–1.05 p.u.) and loading (100%) limits.

Since voltage drop and high line loading are expected to become potential challenges in future distribution grids, the heatmaps in Figure 18 and Figure 19 illustrate, respectively, the minimum magnitude and the maximum line loading observed across the entire network for each scenario and hourly time step in scenario set 3, which comprises 120 scenarios representing operating conditions during the third quarter of the year. Each row corresponds to a scenario, while each column represents an hourly snapshot over the 24-hour horizon. For every scenario and hour, Figure 18 reports the minimum voltage magnitude among all buses, whereas Figure 19 reports the maximum loading percentage among all lines. Consequently, each heatmap cell represents the most critical network condition at a given time step rather than the value associated with a specific bus or line.

The minimum voltage ranges between 0.940 and 0.952 p.u., remaining close to the acceptable lower limit throughout the day, while the maximum line loading varies from 95% to 130%, indicating higher thermal stress in some feeders. Both figures reveal that early morning (0–3 h) and evening (18–22 h) are the most critical periods, where low PV generation and high demand lead to slight voltage drops and line overloads above 100%, confirming the temporal alignment of voltage and thermal congestion. Conversely, during daylight hours (8–15 h), higher PV generation coincides with improved voltage profiles and reduced line loading levels, suggesting that local DER production may contribute to alleviating network stress during these periods.

The relatively uniform color distribution in the voltage heatmap indicates limited variability across scenarios, confirming that minimum voltage level remains stable under different stochastic conditions. In contrast, the line loading profile exhibits more noticeable variations, with some scenarios experiencing significantly higher thermal stress, pointing to the sensitivity of certain feeders to specific demand or generation patterns. Overall, while

voltage congestion risk remains low and the system demonstrates robust voltage stability with headroom for moderate load growth or further DER integration, the occurrence of localized thermal overloads reveals feeder-specific bottlenecks that could limit future expansion. These patterns indicate that, although voltage stability is not expected to pose a major issue under future conditions, line congestion will remain a critical operational challenge, particularly during high-demand periods, necessitating enhanced control strategies, demand flexibility, and network reinforcement to ensure reliable operation.

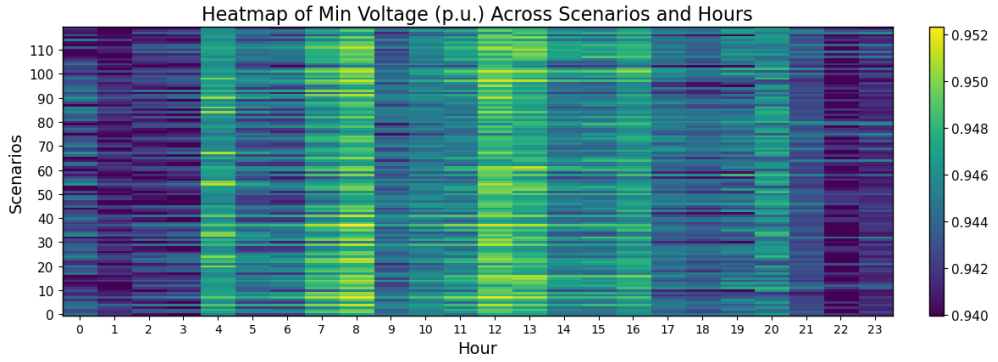


Figure 18. Heatmap of minimum bus voltage (p.u.) across all scenarios and hours in Q3 under Mode 4 operation.

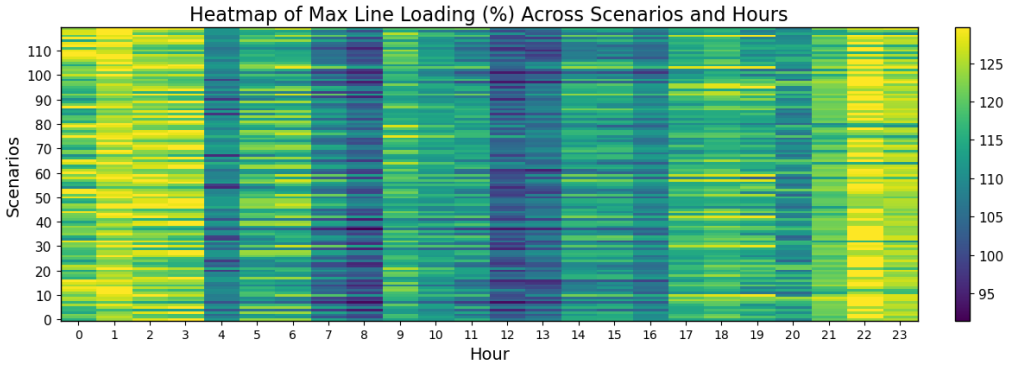


Figure 19. Heatmap of maximum line loading (%) across all scenarios and hours in Q3 under Mode 4 operation.

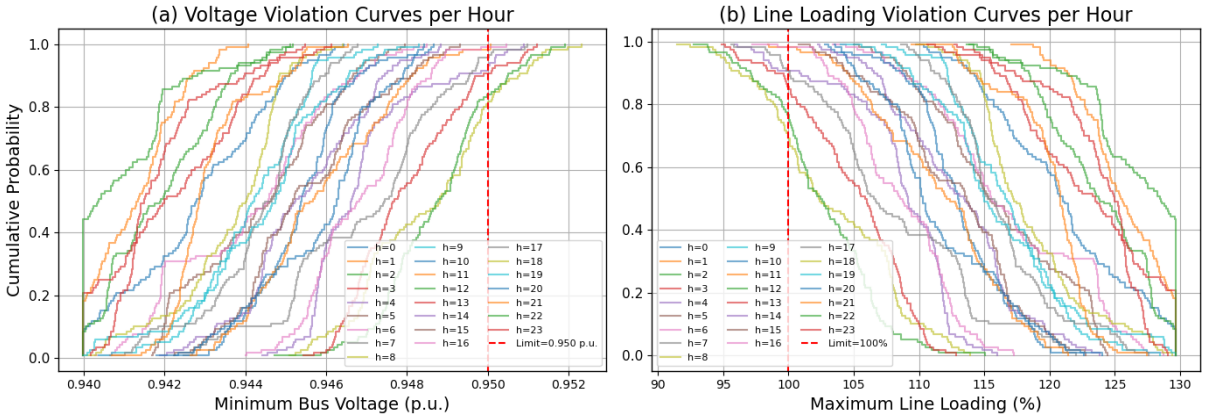


Figure 20. Cumulative probability curves of (a) minimum voltage and (b) maximum line loading violations for each hour across all scenarios in Q3 under Mode 4 operation.

In addition, the MC framework captures these probabilistic variations effectively, which provides a more comprehensive assessment of congestion likelihood and the identification of feeders most prone to overload. Figure 20 presents the minimum voltage and maximum line loading violation probability curves obtained from MC simulations for each hour across all scenarios in Q3 under Mode 4 operation. These curves offer a probabilistic perspective on the network's performance under future load demand growth scenarios.

In subplot (a), most voltage curves cluster close to the 0.95 p.u. threshold, confirming that voltages generally remain within acceptable limits across the several simulated operation scenarios. The position and slope of the curves show that undervoltage events are rare, as only a few scenarios exhibit minimum voltages below the operational limit. Curves corresponding to the early morning (0–3 h) and evening (18–22 h) are slightly shifted to the left, indicating that lower voltage values occur more frequently during these high-demand periods. Conversely, during midday hours (8–15 h), the curves move toward higher voltages. Overall, the results demonstrate strong voltage stability and a low risk of voltage limit violations under the considered future network configuration.

In subplot (b), the line loading violation curves illustrate the distribution of maximum line loading percentages across all scenarios and hours. Several curves extend beyond the 100% thermal limit, particularly during the early morning and evening, when the load demand experience peaks. This pattern indicates that higher loading values occur more frequently during these hours, leading to line congestion in specific network segments. In contrast, during midday hours, the curves shift toward lower loading values due to the lower load demand that reduces upstream power flows and relieves thermal stress. Compared to voltage performance, line loading exhibits greater variability across scenarios, reflecting its higher sensitivity to stochastic fluctuations in demand.

Active power losses (kW)

Line losses are another important indicator for assessing the operational performance and efficiency of electrical distribution grids. They represent the portion of electrical energy dissipated as heat due to the resistance of conductors when current flows through them. In practical terms, line losses are proportional to the square of the current (RI^2). Higher currents typically occur during peak load periods or under congested conditions, leading to greater energy losses and reduced efficiency. Therefore, analyzing line losses provides valuable insight into the thermal loading of lines, network stress levels, and potential congestion points. In this study, losses were calculated from power flow simulations for each line, hour, and scenario, allowing their temporal and spatial variability to be captured under future stochastic demand conditions.

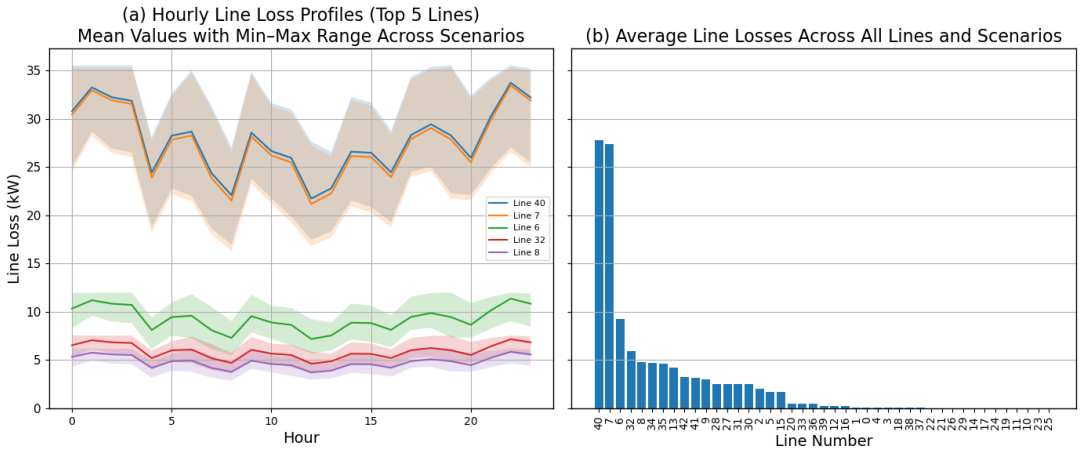


Figure 21. Hourly line loss profiles of the top five lossy lines (a) and average line losses across all lines and scenarios (b).

Figure 21 presents the aggregated results of line loss analysis across all MC scenarios and hours, offering insights into both temporal and spatial loss behavior. Subplot (a) illustrates the hourly line loss profiles of the five lines with the highest average losses, showing the mean hourly values (solid lines) together with the range of variation (min–max shading) across all stochastic realizations. Subplot (b) ranks the average line losses of all lines from highest to lowest, revealing how losses are distributed spatially across the network.

The results indicate that Lines 7 and 8, which are the key feeders connecting one of the main buses (Bus 4) to lower-voltage sections, experience higher and more variable losses, reflecting their crucial role in transferring power between voltage levels. Line 6, located near the main substation, also shows relatively high losses due to its position in handling significant upstream flows. Among all, Line 40 stands out as a major loss contributor since it links the 30 kV and 6.6 kV networks that supply several large load clusters, while Line 32 connects directly to one of the principal loads (CARGA-3) on the 30 kV system. These heavily loaded and structurally critical feeders exhibit both higher average losses and greater scenario-dependent variability, suggesting sensitivity to demand and generation fluctuations and highlighting potential congestion or efficiency bottlenecks. In contrast, the majority of lines show relatively low and stable losses, implying that thermal stress within the grid is localized rather than widespread. Overall, the figure demonstrates that while the network operates efficiently under normal conditions, strategic reinforcement or operational flexibility in a few key feeders could significantly enhance overall efficiency and reduce local congestion, particularly under future operation conditions.

4.4 KPI calculations

To evaluate the outputs and added value of Demo 2, a comprehensive set of KPIs has been defined and classified into two main categories: general KPIs and technical KPIs. The general KPIs were defined within the overall project scope and provided as common evaluation indicators for Demo 2, covering environmental, social, and economic aspects. In contrast, the technical KPIs were selected specifically for the SESST application and the Port of Sines case study, based on commonly used performance indicators in power system operation and distribution network assessment. These indicators aim to quantify the overall performance, impact, and usefulness of the SESST, which integrates scenario generation and grid assessment modules. The KPI framework provides a structured approach to demonstrate how the developed tool contributes to energy system planning, decision-support, and stakeholder engagement.

4.4.1 Technical (Demo-specific) KPIs

As part of the SESST outputs, this section provides a quantitative evaluation of the operational performance of the future MV distribution network using a set of technical KPIs considered most relevant for grid operation, congestion assessment, and network efficiency analysis. These include:

Number of assets operating under congestion [#]

Assets operating under congestion are defined as grid components (lines, transformers, or buses) that violate or approach their operational limits under a given scenario. In this study, congestion is primarily assessed through line thermal overloads and voltage constraint violations; thus, any line with loading above 100% or bus with voltage outside the [Vmin, Vmax] range is operating under congestion. Transformers connected to congested lines or buses are also regarded as indirectly affected assets. **Fout! Verwijzingsbron niet gevonden.** represents the quarterly summary of the number of congested assets and the frequency of congestion for the corresponding asset within a day. The table includes the quarter (Q1–Q4), asset type (lines or buses), the number of scenarios (n) analyzed per quarter, the average number of congested assets per day (mean), and two congestion frequency indicators: mean hours and median hours, which describe how many times the congested assets typically experience congestion within a single day. It is worth noting that the considered future case study comprises a total of 43 lines and 51 buses.

Table 2. Congestion information: number of congested assets, asset type, and duration.

Quarter	n (Scenarios)	Asset Type	Mean (No. of Congested Assets per Day)	Mean Hours (Average Duration of Congestion)	Median Hours
Q1	60	Lines	2	23.64	24.0
		Buses	3	18.24	20.0
Q2	90	Lines	2	23.09	24.0
		Buses	3	16.07	18.0
Q3	120	Lines	2	23.25	24.0
		Buses	3	16.48	18.0
Q4	150	Lines	2	22.82	23.0
		Buses	3	16.82	19.0

The results presented in Table 2 provide a detailed overview of the number and frequency of assets operating under congestion throughout the year. On average, approximately two lines and three buses experience congestion per day across all quarters. This consistency indicates that congestion is concentrated on a limited subset of critical network components that are repeatedly exposed to operational stress. In other words, rather than congestion shifting widely across the network, the same lines and buses tend to be affected persistently, revealing structural bottlenecks within the grid.

Despite the similar number of congested assets across quarters, the frequency of congestion, that is, how often these assets experience congestion during a day, shows seasonal variability. Line congestion remains almost continuous across all quarters, with mean values of around 23 hours per day, suggesting that certain branches are consistently thermally overloaded. This persistent behavior likely reflects high and steady power flows combined with limited network flexibility, implying that these lines operate close to their capacity limits regardless of seasonal changes. In contrast, bus congestion exhibits more pronounced variation over the year, with mean congestion durations ranging between 16 and 18 hours per day. The highest frequency of bus congestion occurs in Q1, which aligns with the winter season when load demand is typically higher due to heating needs. The reduced congestion frequency observed in Q2 and Q3 corresponds to periods of higher distributed generation, particularly from PV

sources, which help support voltage levels and mitigate under-voltage conditions. In Q4, congestion frequency increases again as the system transitions back to heavier loading conditions during the colder months.
The difference between mean hours and median hours in the table further clarifies the nature of congestion dynamics. The mean hours represent the average number of congested hours per day, accounting for all assets and scenarios, and are therefore sensitive to extreme events where certain components may remain congested for unusually long periods. The median hours, on the other hand, indicate the typical congestion duration, offering a more robust measure of the central tendency. When the mean and median values are close, as seen for lines, congestion is relatively uniform across assets and time. However, the larger disparity observed for buses, especially in Q1 and Q4, implies that voltage-related congestion is more intermittent, with some buses experiencing long-lasting issues while others only face short-term violations.

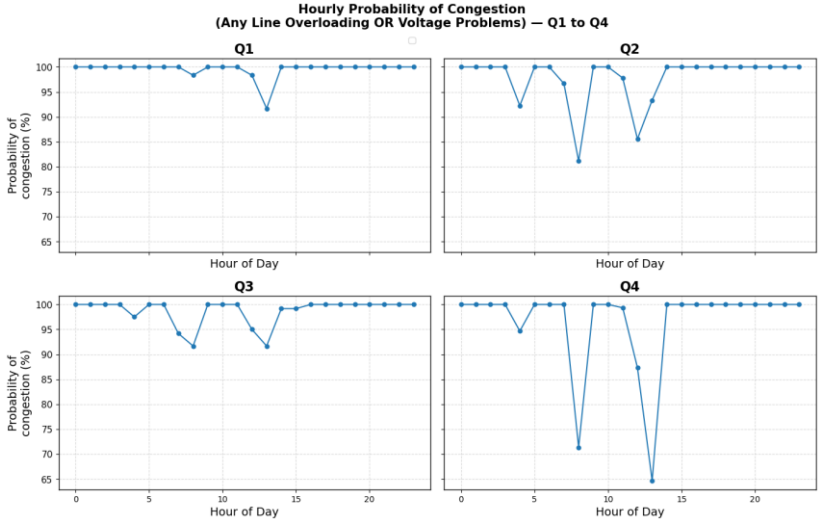


Figure 22. Hourly probability of congestion in the distribution grid across scenarios for each quarter (Q1–Q4).

Figure 22. Hourly probability of congestion in the distribution grid across scenarios for each quarter (Q1–Q4). shows the likelihood that at least one network asset (line or bus) experiences congestion, defined as either thermal overload on any line or voltage violation at any bus, during each hour of the day. Indeed, the figure illustrates how frequently the future distribution grid is expected to experience congestion at different hours of the day, based on a large set of scenarios for four representative quarters of the year. Across all quarters, the probability of having at least one congested asset is extremely high, typically above 95% for most hours, and frequently reaching 100%. This indicates that congestion is not an occasional or rare phenomenon but a structural and persistent characteristic of the network under projected future operating conditions.
Although the probability remains high throughout the day, the curves exhibit hour-dependent fluctuations. These drops in probability correspond to hours during which fewer scenarios produce overloads or voltage issues, typically influenced by expected variations in load demand and renewable generation profiles. For instance, reductions in congestion probability during midday or late-night hours align with periods where demand may be lower or generation more balanced.
The analysis shows that for the considered case study, the probability of experiencing congestion in the future distribution grid is consistently high across all hours of the day and across all seasons, indicating that at least one network component frequently operates close to or beyond its thermal or voltage limits. These results suggest that the analyzed network has limited operational headroom under the assumed future demand and DER penetration levels and is therefore prone to congestion-related constraints.

More generally, the findings highlight the importance of assessing distribution network performance under future uncertainty scenarios. As electrification and DER integration continue to increase, maintaining sufficient operational flexibility and network headroom may become increasingly challenging. Consequently, probabilistic congestion assessment can provide valuable insights for identifying potential bottlenecks and supporting the development of appropriate congestion management measures, flexibility mechanisms, operational planning strategies, and network reinforcement decisions.

Level of Congestion (per asset) [High, Medium, Low]

In addition to identifying how many assets operate under congestion and how frequently they experience such conditions over a day, the severity (or level) of congestion plays a critical role in understanding the actual risk imposed on the grid. Congestion is not a binary phenomenon; the extent to which operational limits are exceeded determines whether the problem can be solved through short-term operational measures or requires more fundamental interventions. Sustained operation under a high level of congestion can accelerate equipment ageing, increase failure probability, and compromise overall network reliability, often necessitating reinforcement, component replacement, or major and costly upgrades. In contrast, mild congestion events are typically manageable through flexibility activation, DER curtailment, or other short-term operational adjustments. To capture the severity of operational stress on the network, congestion is classified into three levels: high, medium, and low, defined as below:

- **High congestion** refers to violations that substantially exceed safe operating margins. For line loading, this corresponds to a loading level above 150% of the thermal rating. For voltage, this corresponds to deviations greater than ±10% from the permissible band (i.e., $V < 0.90$pu or $V > 1.10$ p.u.).
- **Medium congestion** captures moderate violations where operational thresholds are exceeded to a meaningful but not yet critical extent. For lines, this refers to loadings between 120–150% of the thermal limit. For voltage, it corresponds to deviations of ±(5–10)% from the allowable band (i.e., $0.9 \leq V < 0.93$ p.u. or $1.07 < V \leq 1.10$ pu).
- **Low congestion** represents mild exceedances of operational limits. For thermal overloads, this includes loading between 100–120% of the limit, while for voltage, this includes deviations just outside the acceptable range (e.g., $0.93 \leq V < 0.95$ p.u. or $1.05 < V \leq 1.07$).

Table 3. Asset-level congestion severity classification based on average daily behavior

Asset type	Congestion level	Number of assets
Bus	Low	3
Line	Low	2
Line	Medium	2

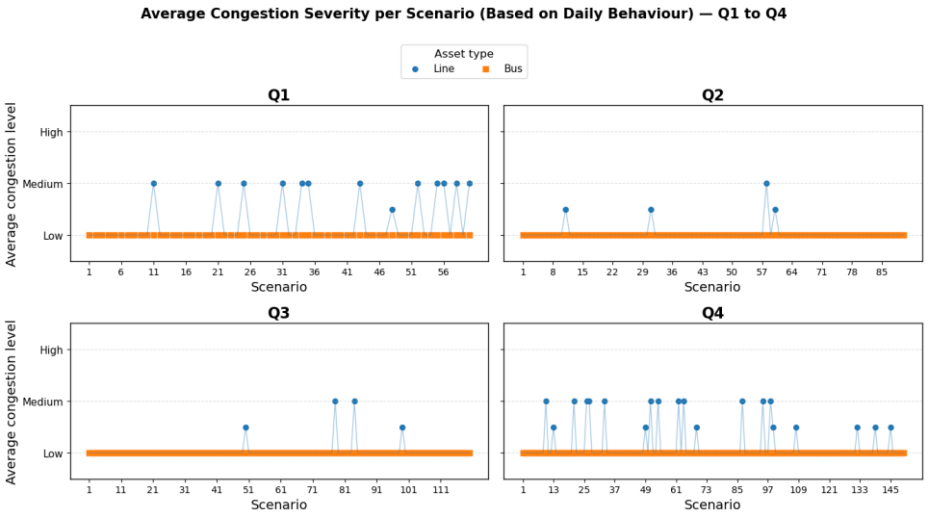


Figure 23. Average congestion severity per scenario for lines and buses across quarters (Q1–Q4).

Table 3 summarizes each asset's overall average congestion level, revealing the structural stress points of the future grid: all buses fall into the low congestion category, indicating only mild voltage deviations, while lines show a split between low and medium severity, reflecting more pronounced but still manageable thermal loading. No asset appears in the high-severity congestion category, indicating that although limits are exceeded, none of the assets experience dangerously extreme congestion conditions.

Figure 23. Average congestion severity per scenario for lines and buses across quarters (Q1–Q4). extends this analysis by showing how average congestion severity varies across scenarios and seasons. As mentioned above all buses consistently fall into the low-severity band across all scenarios and quarters, confirming that voltage issues remain mild and stable over time. Lines, however, display a broader spread, with many scenarios reaching medium severity. As mentioned in the table, no assets reach the high-severity category, further validating that extreme overload conditions do not emerge under the simulated conditions.

For the considered Sines future grid scenario, the results indicate that thermal congestion, rather than voltage deviation, is the dominant operational challenge in the future grid. Voltage issues remain relatively mild and localized, whereas line loading constraints appear more frequently and with greater severity across scenarios. This distinction is crucial for planning effective mitigation measures: targeted management of thermal bottlenecks, rather than broad voltage control, will likely yield the greatest improvement in system performance under high DER penetration. Collectively, the findings show that the future grid is expected to operate under persistent but moderate congestion, with several assets regularly approaching their operational limits without reaching critical or unsafe levels. This underscores the importance of proactive congestion management through flexibility activation, refined operational strategies, and selective reinforcement to maintain reliability as electrification and DER integration continue to expand.

Energy Losses (MWh)

Fout! Verwijzingsbron niet gevonden. illustrates the distribution of daily energy losses across all MC scenarios for each quarter of the year. Each subplot corresponds to one season and displays how total daily losses vary from scenario to scenario based on different realizations of demand. Despite this variability, daily losses remain within a narrow range, varying from ~2.6 MWh to ~3.1 MWh, indicating limited fluctuation in overall system losses. The seasonal averages reinforce this observation: Q1 exhibits the highest average daily loss

at 2.950 MWh, while Q2 shows the lowest at 2.795 MWh, with Q3 and Q4 following closely at 2.824 MWh and 2.843 MWh, respectively.

In addition, Figure 25. Distribution of daily line losses per line across scenarios for different quarters of the year.shows the distribution of daily line energy losses for each network line under all MC scenarios, displayed separately for each quarter. Each boxplot reflects the range of daily losses for a single line, capturing the scenario-driven variability in loading. The results reveal that losses are concentrated in a small number of lines, most notably Lines 6, 7, 8, 41, and 42, which consistently exhibit substantially higher losses across all seasons. In contrast, the majority of lines show losses near zero, and the identity of the high-loss lines remains nearly unchanged from Q1 through Q4, suggesting a strong structural pattern.

For the Port of Sines network, the results show that annual energy losses remain relatively stable despite seasonal variations in demand and DER generation. Although the magnitude of losses varies slightly throughout the year, the majority of losses consistently occur on a small subset of heavily utilized lines, while the ranking of the highest-loss corridors remains largely unchanged across seasons.

More generally, it can be concluded that energy losses in future distribution networks are influenced more strongly by network topology and power transfer patterns than by short-term operating conditions. As a result, a relatively small number of structurally important network elements are likely to account for a disproportionate share of total losses under a wide range of scenarios. Therefore, loss-reduction strategies should prioritize targeted interventions on persistent loss hotspots, such as network reinforcement, asset upgrades, or operational optimization, rather than relying solely on seasonal or system-wide measures.

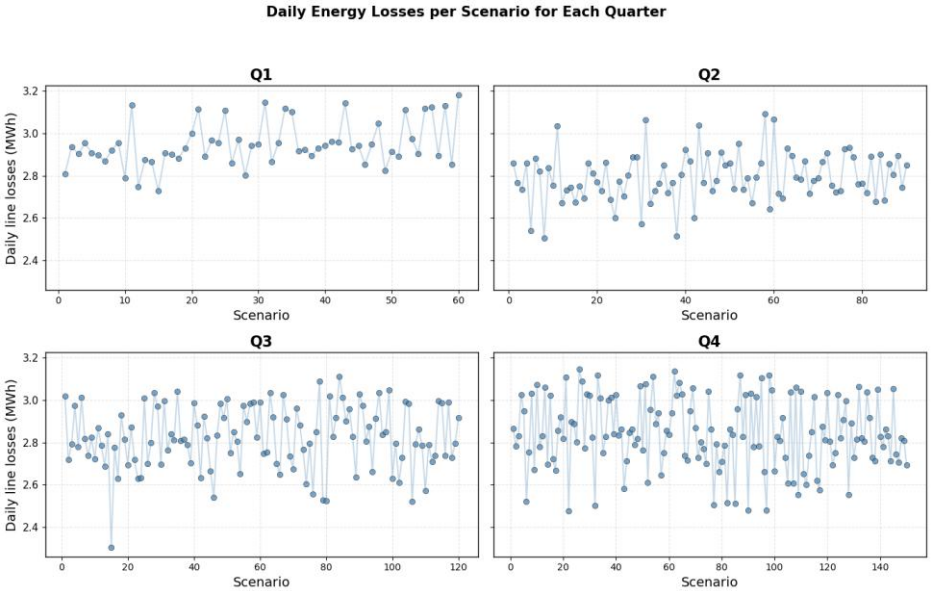


Figure 24. Daily energy losses of the system per scenario across seasons.

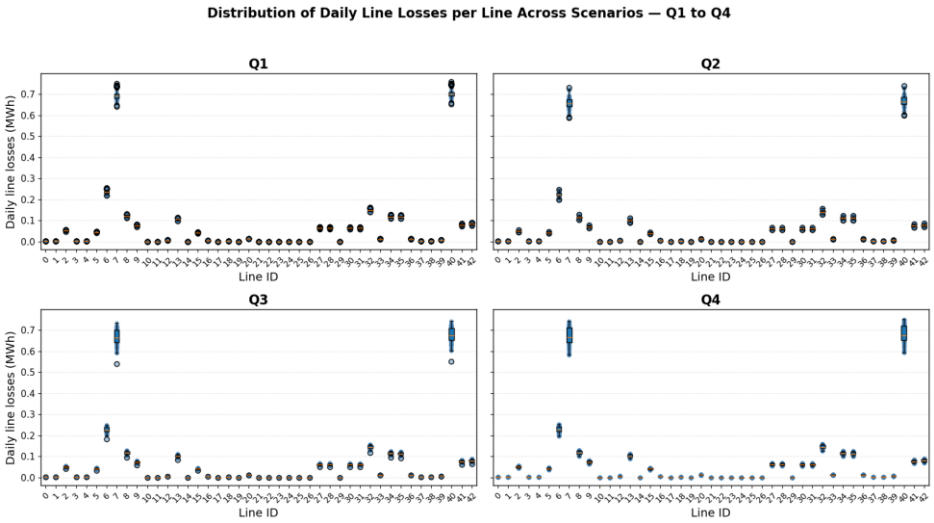


Figure 25. Distribution of daily line losses per line across scenarios for different quarters of the year.

Ratio of self-consumption and self-sufficiency

Self-consumption means how much of the energy produced by local DER is actually used locally (instead of being exported). Closely related is self-sufficiency, which means how much of the local demand is supplied by local DER (instead of imports from the upstream grid). These two can be defined as follows:

Self-consumption (SC): $$SC = \frac{local\ generation\ used\ to\ supply\ local\ load}{total\ local\ generation}$$

Self-sufficiency (SS): $$SS = \frac{local\ generation\ used\ to\ supply\ local\ load}{total\ local\ load}$$

Table 4. Mean self-sufficiency and self-consumption of the grid across quarters.

Quarter of year	Daily energy demand (MWh)	Self-sufficiency-mean (%)	Self-consumption-mean (%)
Q1	830.47	18.94	100.00
Q2	806.77	19.50	100.00
Q3	811.18	19.40	100.00
Q4	813.81	19.34	100.00

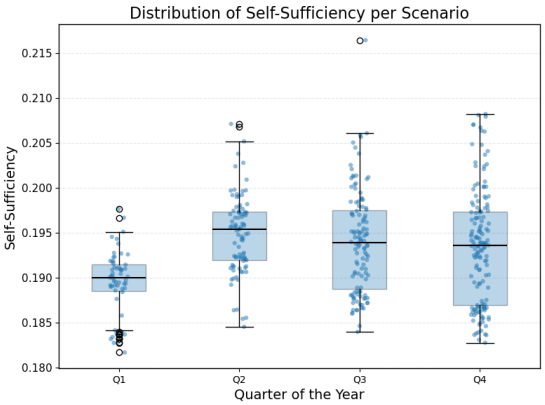


Figure 26. Distribution of self-sufficiency across all scenarios for each quarter (Q1–Q4).

Figure 26 illustrates the distribution of self-sufficiency across all MC scenarios for each quarter of the year, showing how much of the total electricity demand is locally supplied by PV generation embedded within the distribution grid. Although individual scenario points introduce some variability, the overall distribution remains compact for each quarter. Seasonal differences are visible but relatively small, with Q2 (spring) exhibiting slightly higher median of self-sufficiency and Q1 (winter) showing the lowest values. This pattern reflects the seasonal variation in solar availability and load levels. These visual observations are fully consistent with the aggregated results in Table 4, where the mean self-sufficiency ranges from 18.94% in Q1 to 19.50% in Q2, confirming that seasonal effects influence local contribution but only moderately.

In addition, Table 4 also shows that self-consumption remains at 100% for all quarters, indicating that every unit of PV generation generated within the grid is consumed locally and no surplus is exported to other networks. It means while the grid makes full and efficient use of its available PV generation, the installed solar capacity is relatively small compared to total demand. As a result, self-sufficiency remains low but stable across the year, highlighting a system in which local renewable generation is fully utilized but insufficient to substantially offset overall consumption.

More generally, self-sufficiency and self-consumption indicators provide valuable insights into the extent to which local renewable generation can support local demand. While self-consumption reflects the effectiveness of utilizing locally generated energy, self-sufficiency indicates the contribution of local generation to overall electricity needs. These metrics help identify whether future increases in renewable capacity should focus on expanding generation resources, improving demand-side flexibility, or integrating energy storage solutions to further reduce dependence on external energy supply.

Renewable Energy Curtailment [%, kW]

Renewable curtailment refers to the amount of renewable energy that was available in the grid but not injected because of network or operational constraints. It can be calculated for each time step as:

$$E_{curt,t} = E_{avail,t} - E_{inj,t}$$

And, over a day:

$$Curtailment\ rate = \frac{\Sigma_t E_{curt,t}}{\Sigma_t E_{avail,t}}$$

In the case of the 30 kV Port of Sines network, renewable generation remains well below the hosting capacity of the grid. With only 250 kW of initial RES installation and 6.3 MW in the expanded scenario, all available power is fully injected without any curtailment. This result

is consistent with the previously observed 100% self-consumption, indicating that local demand is sufficient to absorb all generated renewable energy. This indicates that the network can accommodate significantly higher levels of RES integration. Consequently, the results suggest that additional PV capacity could be integrated into the system. However, detailed planning studies would be required to determine the optimal sizing and siting of future installations.

More generally, renewable curtailment serves as an indicator of the extent to which network or operational constraints limit the utilization of available renewable resources. Low or zero curtailment suggests that the existing grid infrastructure can accommodate the installed renewable capacity, whereas increasing curtailment may signal the need for network reinforcement, operational flexibility measures, energy storage, or alternative connection strategies. As such, curtailment analysis provides a useful tool for assessing renewable hosting capacity and identifying potential barriers to future renewable energy integration.

Cost of Congestion [€]

The cost of congestion is a broad concept and can refer to different types of economic impacts that arise when a distribution grid reaches or exceeds its operational limits. In general, congestion costs can be interpreted in three complementary ways:

- Operational congestion cost: the short-term, real-time cost of managing overloads or voltage issues (e.g., dispatching flexibility, reconfigurations, curtailment, or other interventions).
- Asset stress / degradation cost: the long-term cost associated with accelerated wear of network components when operated close to or beyond their thermal limits.
- Reinforcement / investment cost: the strategic cost of upgrading network assets when congestion persists over time.

Accordingly, a general formulation for cost of congestion can be written as following, in which $C_{deg,t}$ is the asset degradation cost, $C_{op,t}$ is the operational congestion cost, and C_{reinf} is the annualized reinforcement cost.

$$C_{cong} = \sum_{t} \left(C_{op,t} + C_{deg,t}\right) + C_{reinf}$$

Since the goal of Demo 2 is to analyze the operational behavior of the future grid, the relevant KPI is the operational congestion cost. This cost captures the value of real-time scarcity in the network and reflects the amount of grid capacity that users occupy during congested periods. Because operational congestion is caused by short-term variations in load and DER behavior, this cost naturally becomes dynamic and time-dependent. This cost should be paid by the actors responsible for the congestion, high-demand consumers during peak hours, or DERs generating surplus energy that drives reverse flows, depending on the scenario. In the Port of Sines case, renewable penetration is still low (250 kW initially and 6.3 MW in the expanded case), and simulation results show no RES curtailment, meaning the grid could still accommodate more PV. Therefore, operational congestion cost would mainly be attributed to large consumers whose demand pushes the grid towards or beyond its limits.

In this Demo, congestion is defined purely from an operational standpoint: the grid is considered congested whenever the power demand or generation causes any line to reach or exceed its thermal loading limit (100%). This ensures that the congestion assessment reflects the actual physical limits of the Port of Sines network under realistic operating conditions. For each line L in the base network, a thermal rating is computed based on its nominal voltage and maximum current:

$$S_L^{max} \approx \sqrt{3} V_L^{nom} I_L^{max}$$

To obtain a representative network capacity, we select the maximum line rating:

$$S^{ref} = \max_{l}(S_l^{max})$$

For each hour t and scenario s, the MC results provide the maximum line loading:

$$L_{t,s}^{max}[\%]$$

Any loading above the admissible limit (100%) is interpreted as a violation of thermal constraints. The overloaded power is therefore estimated as:

$$P_{t,s}^{over} = \max\left(0, \frac{|L_{t,s}^{max} - 100|}{100} S^{ref}\right)$$

This expression scales the excess loading percentage by the representative line capacity, calculating an approximate value of overloaded power in MW. Assuming one-hour time steps ($\Delta t = 1\ h$), the total congested energy in scenario s for a full day is:

$$E_s^{\text{cong, day}} = \sum_{t=1}^{24} P_{t,s}^{\text{over}}\, \Delta t$$

Using a fixed congestion price of 50 €/MWh (tarifas-se_2024.xlsx), the daily congestion cost becomes:

Fout! Verwijzingsbron niet gevonden. illustrates the distribution of daily congestion costs calculated across all scenarios for each quarter of the year, revealing how operational congestion evolves under seasonal variations in demand patterns. In all quarters, congestion costs remain significant, ranging between 12 k€/day and 28 k€/day. Q1 exhibits the highest average daily congestion cost (22.63 k€/day), driven by generally higher winter load levels that stress the network more frequently. Q2 shows the lowest mean cost (18.95 k€/day), reflecting reduced loading conditions typical of spring. Q3 and Q4 present intermediate values, with wider variability due to more diverse daily demand patterns. Table 5 confirms these observations, summarizing the quarterly mean, standard deviation, and min/max values. Together, the results indicate that operational congestion cost is not negligible throughout the year, with winter conditions causing the most persistent stress on the grid.

More generally, congestion cost provides a useful indicator of the operational impact of network constraints and the relative severity of congestion across different operating conditions. It should be noted that the reported values depend on the congestion cost coefficient adopted in the analysis and therefore should not be interpreted as the actual economic cost incurred by the network or its users. Instead, the metric serves as a comparative measure of network stress, enabling the identification of periods and scenarios in which congestion becomes more critical. Consequently, congestion cost analysis can support the assessment of network resilience, the identification of persistent bottlenecks, and the prioritization of future reinforcement, flexibility, or operational measures.

Table 5. Summary statistics of daily congestion cost per quarter.

Quarter of year	Mean cost (k€/day)	Std dev (k€/day)	Min cost (k€/day)	Max cost (k€/day)
Q1	22.63	2.54	17.49	28.16
Q2	18.95	2.75	12.65	26.03
Q3	19.62	3.56	7.79	26.45
Q4	20.15	3.95	11.75	27.34

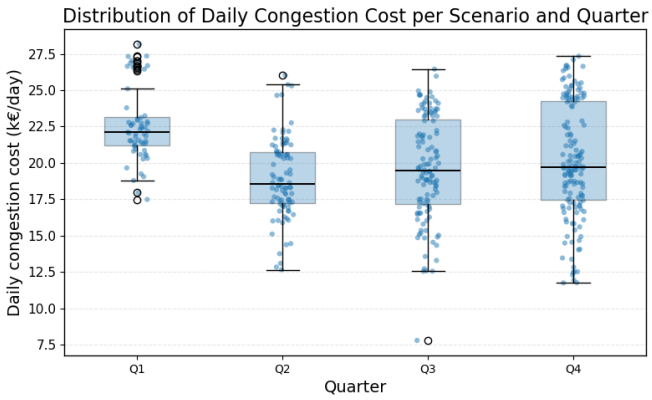


Figure 27. Distribution of daily congestion cost per scenario for each quarter.

4.4.2 General KPIs

The general KPIs reflect the broader environmental, operational, and socio-economic impacts of Demo 2 in alignment with the WP8 monitoring framework. While many metrics in that framework, such as CO_2 emissions per transport activity, pollutant emissions, bunker sales, or land use, are not directly applicable to the software-based developments of Demo 2, several relevant dimensions can still be evaluated to assess the added value of this Demo, including:

Environmental aspects

Although Demo 2 is not directly aimed at decreasing the use of fossil fuels or expanding the adoption of green fuels, its indirect contribution to decarbonization can be assessed through the level of self-consumption and self-sufficiency from RES (e.g., PV generation) and the corresponding impact on emission reductions.

A higher rate of self-consumption and self-sufficiency generally implies a reduced dependence on externally supplied, fossil-fuel-based electricity, thereby supporting broader carbon reduction and sustainability objectives. Furthermore, comparing the total grid power consumption, both in the current and the extended grid configurations considering future load demand growth scenarios, and analyzing the self-consumption levels in both cases can provide valuable insights into indirect environmental KPIs that Demo2 can assess.

Table 6. System-level active load demand, local renewable generation, and indicative power-based renewable contribution ratios across the four operational modes of the base-case network configuration.

Mode	Load demand (MW)	Local generation (MW)	Renewable utilization (%)	Relative local generation share (%)
1	1.16	0.25	1.0	0.21
2	19.34	0.25	1.0	0.01
3	20.16	12.85	1.0	0.63
4	38.34	12.85	1.0	0.33

Future load demand is expected to increase significantly due to multiple factors, including industrial expansion, electrification of port operations, and the integration of emerging "green" technologies. Although these technologies support decarbonization, many of them, such as electric vehicle charging, port equipment electrification, or hydrogen electrolysis, introduce substantial additional electricity demand. As a result, even a transition toward cleaner energy carriers can temporarily elevate the load imposed on the grid. From an environmental perspective, the impact of this increased demand depends largely on the

composition of the generation portfolio: if demand growth is met by RES, the associated emissions remain low; however, if external fossil-based electricity is required to cover the shortfall, the environmental footprint increases.

The scenario-based quarterly analysis in Table 4 and the base-case operational mode results in Table 6 provide complementary insights into the environmental implications of evolving load demand within the Port of Sines electrical infrastructure. The seasonal scenario analysis (Table 4), based on 24-hour simulations throughout the year, shows that the system consistently achieves 100% self-consumption of available renewable generation, while the mean self-sufficiency remains relatively low (approximately 19%) because the total daily energy demand substantially exceeds the renewable energy generated. This indicates that, although all locally generated renewable energy is utilized, a significant share of the electricity demand must still be supplied by external sources.

It should be noted that the indicators reported in Table 6 differ from those presented in Table 4. Whereas Table 4 reports energy-based self-consumption and self-sufficiency metrics obtained from time-series simulations, Table 6 provides a power-based comparison of local renewable generation and load demand across the different operational modes. Therefore, the values in Table 6 should be interpreted as indicative generation-to-load ratios rather than energy-based self-sufficiency indicators.

The results in Table 6 illustrate how network configuration affects the balance between local load demand and installed renewable generation capacity. Mode 1, representing the isolated existing network, exhibits relatively low demand and limited renewable generation, resulting in a modest generation-to-load ratio. Mode 2 connects the 30 kV network to the lower-voltage grids, leading to a substantial increase in demand while renewable generation remains unchanged, thereby reducing the relative contribution of local generation. Mode 3 demonstrates the impact of the extension areas, where the addition of new renewable generation significantly improves the generation-to-load ratio. Finally, Mode 4, in which all connections and extensions are active, combines expanded renewable generation with substantially higher demand. Although local renewable capacity increases compared to the existing network, the growth in demand remains proportionally larger, highlighting the need for additional renewable deployment if a higher level of energy autonomy is desired.

By quantifying how changes in load profiles, grid topology, and renewable integration affect self-consumption, self-sufficiency, and reliance on external (potentially fossil-based) supply, Demo 2 enables stakeholders to evaluate the indirect decarbonization benefits of grid extensions and renewable deployment. The findings consistently show that while the current and planned RES installations contribute positively to the port's sustainability objectives, substantial further renewable integration will be required to cover the increasing electricity demand driven by industrial activity and the electrification of port operations.

Operational aspects

Demo 2 is mainly an energy infrastructure and grid performance demonstration, not a logistics or fuel-sales one. Therefore, Demo 2 does not directly address most of the port operational KPIs. However, Demo 2 significantly contributes to the understanding of port energy reliability, a key operational KPI, by evaluating whether the Port of Sines' electrical grid can maintain stable and secure operation under future load demand growth and increasing renewable integration. The analysis of different grid configurations (Modes 1–4) demonstrates how connectivity, DER generation, and load expansion influence the availability of power for essential port activities.

Furthermore, Demo 2 does not explicitly model charging behavior or battery performance. However, by quantifying available grid capacity, congestion levels, and renewable self-consumption, Demo 2's results can be insightful into the port's ability to support fast-charging infrastructure for electric mobility and the potential effectiveness of battery storage for peak

shaving and renewable utilization. The results of Demo 2 can indirectly support MAGPIE's broader operational objectives by helping ensure that the future electrified and digitalized port remains reliable, resilient, and environmentally sustainable.

Socio-economic acceptance

Economic KPIs

Demo 2 provides quantitative insight into several economic KPIs, including added value, OPEX/CAPEX, and the economic feasibility of DER deployment. It should be noted that the added value indicator represents the daily operational added value of local renewable generation and does not constitute a full techno-economic investment assessment, as CAPEX and OPEX of additional DER assets are not included. The analysis of the four operational modes shows how much of the load is supplied by local renewable generation and how much must be imported from the external grid, which forms the core of the economic assessment. In all operational modes, the self-consumption ratio of renewables is 100%, meaning all local PV/DER generation directly offsets purchased electricity. For each mode:

$$E_{SC,t} = E_{RES,t} \quad E_{imp,t} = E_{load,t} - E_{SC,t}$$

From the results given by Table 6:

- Mode 1:
  - Total load demand ≈ 1.16 MW, local RES generation ≈ 0.25 MW
  - Imported power (Indicative net demand based on the installed local generation capacity) $P_{\text{imp,1}} = 1.16 - 0.25 = 0.91$ MW
  - The ratio of load covered by imports ≈ $0.91/1.16 \approx 78\%$
- Mode 2:
  - Total load demand ≈ 19.34 MW, local RES generation ≈ 0.25 MW
  - Imported power $P_{\text{imp,2}} = 19.34 - 0.25 = 19.09$ MW
  - The ratio of load covered by imports ≈ $19.09/19.34 \approx 99\%$
- Mode 3:
  - Total load demand ≈ 20.16 MW, local RES generation ≈ 12.85 MW
  - Imported power $P_{\text{imp,3}} = 20.16 - 12.85 = 7.31$ MW
  - The ratio of load covered by imports ≈ $7.31/20.16 \approx 36\%$
- Mode 4:
  - Total load demand ≈ 38.34 MW, local RES generation ≈ 12.85 MW
  - Imported power: $P_{\text{imp,4}} = 38.34 - 12.85 = 25.49$ MW
  - The ratio of load covered by imports ≈ $25.49/38.34 \approx 66\%$

Table 6 shows that Modes 1 and 2 rely predominantly on external electricity supply due to the limited amount of local renewable generation. In contrast, Modes 3 and 4 exhibit a substantially greater contribution from local generation owing to the integration of additional DERs in the extension areas. The values reported in Table 6 are derived from

aggregate load demand and installed renewable generation capacities and are intended to provide a high-level comparison of the relative contribution of local renewable generation across the different operational modes. They should not be interpreted as simultaneous operating conditions or actual imported power levels.

If $p_t^{\text{grid}}$is the electricity price, the energy-related added value of Demo 2's RES deployment over a period is:

$$Added_value_{energy} = \sum_t E_{SC,t} \cdot p_t^{grid}$$

$E_{\text{SC},t}$ is already calculated from the PF results, and multiplying it with prices converts this directly into euros. For example, if a fixed electricity price of P^{grid}=100(€/MWh) is assumed, the added values in Table 7 can be obtained in each operation modes. This shows that operational modes with higher DER integration (Modes 3 and 4) generate substantially higher economic value. The quarterly analysis (Table 4) shows that average self-sufficiency is only ~19% over the year, so ~81% of daily demand is still imported. This means there is significant economic headroom for further DER deployment: additional PV/DER would still likely be highly valuable because it would continue to displace relatively expensive imports rather than being curtailed.

Table 7. Estimated Added Economic Value from Self-Consumed Renewable Energy Under Different Operational Modes.

Operation Mode	Self-consumed RES (MW)	Added value (€/h)
1	0.25	25
2	0.25	25
3	12.85	1,285
4	12.85	1,285

Cost of Imported Electricity (OPEX component):
OPEX refers to recurring costs required to operate and maintain the system. For electrical systems, OPEX mainly depends on imported energy, technical losses, and operation and maintenance (O&M) costs for DERs.

$$OPEX_{energy} = \sum_t P_{imp,t} \cdot p^{grid}$$

Imported power per mode directly determines OPEX. Modes 2 and 4 (the operation modes in which 30 kV network is connected to other parts of Port of Sines) have the highest operational cost due to large external energy dependency.

Cost of Technical Losses (OPEX component):
Demo 2 provides as part of its results, line losses and transformer losses.

$$OPEX_{loss} = \sum_t P_{loss,t} \cdot p^{grid}$$

Loss-related OPEX rises notably in Modes 2 and 4, where loading is highest.

O&M Costs for DER (OPEX component):

$$OPEX_{DER} = \sum_i P_{RES,i} . C_{RES}^{O\&M}$$

Typical assumptions:

- PV O&M cost: 10–15 €/kW-year
- Storage O&M cost: 1–2% of CAPEX per year

Mode 3 and Mode 4 carry higher DER OPEX due to 12.85 MW installed PV/DER.

CAPEX

CAPEX represents one-time investments required for new infrastructure or upgrades. Demo 2 identifies exactly where these arise.

Grid Reinforcement CAPEX

a) When line or transformer loading exceeds acceptable limits:

$$CAPEX_{line} = \Delta L_{\ell} \cdot c^{line}, \qquad CAPEX_{trafo} = \Delta S_k \cdot c^{trafo}$$

Where:

- ΔL_{ℓ}: required new line length or conductor upgrade
- ΔS_k: transformer capacity reinforcement

Modes 2 and 4 indicate the highest reinforcement needs.

b) CAPEX for New DER (PV, wind or storage):

$$CAPEX_{PV} = P_{PV} \cdot c^{PV}, \qquad CAPEX_{storage} = E_{stor} \cdot c^{stor}$$

Typical values:

- PV: 600–1000 €/kW, Batteries: 150–300 €/kWh

Mode 3 and 4 include 12.85 MW of PV/DER , which results in directly scalable CAPEX.

CAPEX for Flexible Assets

(e.g., EV chargers, hydrogen electrolysers, smart inverters)

$$CAPEX_{flexibility} = \sum_{a} P_a \cdot c_a$$

Social acceptance

Beyond economic metrics, Demo 2 plays an indirect but important role in supporting social KPIs, especially within the MAGPIE framework on social acceptance and spatial impact. Although the tool itself does not measure stakeholder attitudes, its technical outputs provide the clarity and transparency needed to improve the understanding of renewable energy installations, grid expansion needs, and the environmental benefits of increased electrification. Social acceptance depends heavily on perceived usefulness, ease of integration, and awareness of risks or nuisances associated with new technologies. By illustrating the system-wide impacts of DER installations and load growth, such as reduced emissions, increased local generation, and improved network resilience, Demo 2 provides a strong evidence base that can support communication, awareness-building, and decision-making among local communities, industries, and authorities. Additionally, the spatial implications of new energy infrastructure, including land use and physical connections, can be better assessed when the technical requirements are clearly mapped, making Demo 2 a supportive tool for broader spatial planning and stakeholder discussions.

Finally, the implementation and governance requirements of Demo 2 are themselves linked to socio-economic acceptance. To use the tool correctly, users need a minimum level of technical expertise in power systems, DER integration and KPI interpretation. In practice, this means that grid operators and technical staff can work directly with the model, while other stakeholders (investors, port planners, large customers, policymakers) benefit from derived indicators, dashboards and explanatory material rather than raw PF outputs. Specifying these training needs and user roles is part of the KPI framework: it clarifies whether "anyone" can use the tool or whether expert mediation is required.

Clear data ownership and data-sharing arrangements are also essential. Demo 2 relies on detailed grid data, load profiles, and DER characteristics. Agreeing on who owns these data, how they can be shared (e.g. via a secure platform), and how results may be used is a prerequisite for wider uptake beyond the core technical team. Establishing robust governance, including validation procedures with industry and port stakeholders, not only improves the technical credibility of the model but also supports social acceptance and investor confidence. In this way, Demo 2 becomes more than a technical prototype: it evolves into a decision-support tool that links economic performance, social acceptance, and practical implementation requirements for future low-carbon developments in ports. Future enhancements could further increase its value by enabling stakeholders to interactively explore alternative energy-transition pathways, modify key assumptions and deployment scenarios, and directly assess the resulting impacts on network operation, renewable integration, and economic performance.

5. Conclusions & Next steps

Demo 2 developed a comprehensive SESST integrating a scenario generation tool and a grid assessment module capable of evaluating present and future operating conditions of the case study (Port of Sines) electrical network. The tool successfully demonstrated its ability to generate realistic demand scenarios, run extensive MC–based load flow analyses, quantify congestion risks, and compute a wide range of technical and economic KPIs. These capabilities enable a rigorous assessment of flexibility requirements, operational bottlenecks, and investment needs under the port's ongoing energy transition. The SESST framework can be readily extended, if required, to capture additional energy-transition pathways beyond those considered in this study, including different levels of port electrification, shore power adoption, hydrogen deployment, alternative vessel fuels, and other emerging technologies that may significantly influence future electricity demand and network operation. Although the framework was developed and validated using the Port of Sines as a case study, its underlying methodology is generic and scalable, enabling straightforward adaptation to a broad range of electrical distribution systems, including industrial sites, energy communities, campuses, airports, logistics hubs, and other infrastructures undergoing electrification and renewable energy integration.

From a technical perspective, the tool revealed that the future 30 kV network will maintain strong voltage stability, with voltages remaining within acceptable limits across most scenarios. In contrast, line congestion emerges as a persistent challenge, with several feeders repeatedly exceeding 100% loading and some reaching medium congestion severity. Congestion persists for 20–24 hours per day across all quarters, indicating structural bottlenecks in specific lines. Energy losses remain stable (2.8–3.0 MWh/day), and renewable integration shows full self-consumption but low self-sufficiency (~19%), suggesting substantial remaining hosting capacity for additional RES integration. Furthermore, the tool provides valuable insights into where targeted reinforcements, operational flexibility, and improved network control will be required. These findings provide decision-support information for the Port of Sines and other stakeholders by identifying network bottlenecks, informing

reinforcement planning, evaluating flexibility options, and supporting future investment decisions for grid expansion and electrification.

Beyond the specific findings for the Port of Sines case study, the application of the SESST provided several methodological insights. The results demonstrate that the combination of scenario generation and MC-based load-flow analysis is effective for identifying structural network bottlenecks, quantifying uncertainty-related risks, and assessing the impact of future load growth and DER integration on network performance. The framework proved particularly suitable for long-term planning studies, where multiple future development pathways and uncertain operating conditions must be evaluated. At the same time, the study highlighted several limitations. While the tool can successfully identify congestion risks, hosting capacity constraints, and reinforcement needs, it does not currently determine optimal mitigation actions, such as DER curtailment strategies, storage dispatch, network reconfiguration, or flexibility activation. These aspects would require the integration of optimization-based congestion management modules. Furthermore, the quality of the results depends on the availability and accuracy of demand, generation, and network data, as well as the representativeness of the future scenarios considered. Overall, the SESST provides a robust and scalable framework for network assessment under uncertainty and can support strategic planning decisions across a wide range of electrical infrastructures.

From an economic KPI viewpoint, the simulator quantified added value, CAPEX needs, and economic feasibility of DER deployment (OPEX). Modes including significant PV self-consumption (Modes 3 and 4) generated approximately €1,285/hour in added value (based on €0.10/kWh), compared to €25/hour in Modes 1 and 2. These results confirm that integrating local PV significantly increases operational value while reducing energy procurement costs. CAPEX requirements identified for the Port of Sines are primarily associated with the reinforcement of critical feeders (e.g., lines 11, 12, 20, 24, 35, and 36). In addition, the SESST framework provides a methodology for estimating future investment requirements related to DER and storage deployment, although project-specific PV and storage expansion costs were not explicitly assessed within the scope of the present study. . OPEX impacts are modest, driven primarily by consistent line losses and potential operational congestion management. Importantly, no renewable curtailment was observed, indicating strong economic feasibility for further DER expansion.

In terms of social acceptance and broader system value, Demo 2 supports coordinated planning among DSOs, port authorities, industrial consumers, and energy communities. By visualizing congestion, flexibility potential, and future operational risks, SESST offers stakeholders a transparent tool to understand system limitations and jointly plan investments. The simulator also aligns with policy goals for digitalization, decarbonization, and community-based renewable energy, providing evidence to support green-port initiatives and improved stakeholder dialogue.

Finally, several prerequisites for the effective deployment of Demo 2 can be identified. Users should have a basic technical background in power flow analysis, Pandapower modeling, and data handling. Clear data governance, including data ownership, access protocols, and standardized formats, is essential for replicability and scalability across other ports. Institutional support, capacity building, and collaboration with a dedicated technical liaison (e.g., the DSO or port engineering team) can further improve assumption validation and consistent tool application. The modular and scalable framework also enables future extensions, if required, including:

- Integrating congestion management optimization (e.g., DER curtailment, storage dispatch, network reconfiguration).
- Extending DER models and including future technologies (hydrogen, e-mobility charging clusters, OPS growth).

- Enhancing the economic module with full CAPEX/OPEX modeling and long-term cost–benefit analysis.
- Adding a user-friendly interface to facilitate adoption by non-expert stakeholders.